2010-01-01

Chromium(III/VI) Binding To Magnetite (Fe3O4), Hausmannite (Mn3O4), And Jacobsite (Mnfe2O4) Nanomaterials

Jeffrey Edward Hernandez
University of Texas at El Paso, jehernandez5@miners.utep.edu

CHROMIUM(III/VI) BINDING TO MAGNETITE (Fe_3O_4), HAUSMANNITE (Mn_3O_4), AND JACOBSITE ($MnFe_2O_4$) NANOMATERIALS

JEFFREY EDWARD HERNANDEZ

Department of Chemistry

APPROVED:

_____
Jorge Gardea-Torresdey, Ph.D. Chair

_____
Jose R. Peralta-Videa, Ph.D.

_____
Elizabeth J. Walsh, Ph.D.

_____
Patricia D. Witherspoon, Ph.D.
Dean of the Graduate School

Dedication

To GOD the father almighty

To my beloved Beatrice

To my mother Margarita, my sister Lorraine and my entire family

"Science can purify religion from error and superstition;

religion can purify science from idolatry and false absolutes.

Each can draw the other into a wider world, a world in which both can flourish....

We need each other to be what we must be, what we are called to be."

Pope John Paul II

CHROMIUM(III/VI) BINDING TO MAGNETITE (Fe_3O_4), HAUSMANNITE (Mn_3O_4), AND JACOBSITE ($MnFe_2O_4$) NANOMATERIALS

By

JEFFREY HERNANDEZ, B.S.

THESIS

Presented to the Faculty of the Graduate School of

The University of Texas at El Paso

in Partial Fulfillment

of the Requirements

for the Degree of

Master of Science

Department of Chemistry

THE UNIVERSITY OF TEXAS AT EL PASO

August 2010

Acknowledgments

I want to give my sincerest thanks to my advisor and my mentor Dr. Gardea-Torresdey for his guidance and his commitment in helping me achieve my dreams. He is everything a good mentor should be and a fine example of what a true leader should be. I would also like to thank Dr. Peralta for showing me the value of patience and understanding and showing me great kindness in my academic growth and for helping me time and time again with my research. I am also grateful for Dr. Walsh for her time and efforts in reviewing my thesis and agreeing to be on my committee. I would also like to extend my gratitude to Dr. Jason Parsons for his help in my research, for his support in decision making in my projects, but most of all for his pushing me to give 100% effort in my work. I wish to thank Dr. Gardea's research group for all their support, and friendship. I would like to thank especially Christina Gonzalez and Yong Zhao for their aid in many of my research endeavors.

I would like to extend a special thanks to my family especially my mother and sister for their unending support and advice that proved very useful during good time and bad throughout the duration of my academic career. Most of all I would like to thank my beloved Beatrice, my future spouse for her never-ending support, her positive thinking and most of all her unconditional love. I thank her for her patience with me during the rough times when it seemed that I was going to give up on my future; because of her I am now accomplishing my dreams.

I would like to acknowledge the financial support of the National Science Foundation and the EPA for providing the NSF-EPA Agreement #EF 0830117 grant for funding of this project. The authors would also like to thank the United States Department of Agriculture for the USDA grant # 2008-38422-19138 used to fund this project. I would like to thank the Dudley family for Dr. Gardea-Torresdey's Endowed Research Professorship in Chemistry. Portions of this

research were carried out at the Stanford Synchrotron Radiation Laboratory, a national user facility operated by Stanford University on behalf of the U.S. Department of Energy, Office of Basic Energy Sciences. The SSRL Structural Molecular Biology Program is supported by the Department of Energy, Office of Biological and Environmental Research, and by the National Institutes of Health, National Center for Research Resources, Biomedical Technology Program.

Abstract

Chromium is a very versatile metal that is used for many applications in the world. Two of the most common ions of chromium that occur naturally are Cr(III) and Cr(VI). These two oxidation states have very different heath effects in living organisms. Cr(III) is relatively non-toxic to living organisms; however, Cr(VI) is very toxic to most living organisms This study was conducted to find a simple and cost effective method to sequester these two common ionic species of chromium from sources of water that are adjacent to or that are affected by other water sources contaminated by these two ions. In this study an investigation was conducted to observe the binding between three different engineered nanomaterials (Magnetite, Hausmannite and Jacobsite) to both hexavalent and trivalent chromium. A traditional synthesis was used to make these nanomaterials, which consisted of a titration of iron(II) chloride for the Magnetite, manganese sulfate for the Hausmannite, and a combination of the two previous salts in a 2:1 ratio for the Jacobsite. Magnetite (Fe_3O_4) and Hausmannite (Mn_3O_4) were synthesized using two different aging processes and Jacobsite ($MnFe_2O_4$) was synthesized using only one process. The first aging process involves a traditional heating source in an open vessel at 90ºC for 60 minutes. The second ageing technique used was a microwave assisted hydrothermal synthesis method using a closed vessel at 90ºC for 30 minutes. The Jacobsite was aged using only the microwave technique.

The batch studies showed that the binding to the three different materials were pH dependent. The studies showed that Cr(III) and Cr(VI) bind to the nanomaterials differently at different pHs. In addition, the binding of the Cr(III) to the nano-Magnetite showed identical behavior binding to both the open vessel and the hydrothermally synthesized nanoparticles with pH. But the Cr(VI) showed differences in the binding to the open vessel and the closed vessel nano-Magnetite, with higher binding at lower pHs observed with the open vessel nanomaterials

compared to the closed vessel nanomaterials. The Hausmannite micro-waved aged material had a better affinity for the hexavalent chromium then the open aged system. The studies with Cr(III) showed that the ion had greater affinity with the Hausmannite material than with Cr(VI). The Jacobsite showed favorable binding to Cr(VI) then it did to Cr(III) at higher pHs. The studies showed that all the materials exhibited the majority of their binding to chromium at around pH 4. Further data was obtained from batch studies included time dependency, isotherm capacities and interference studies. Overall the nanomaterials adsorbed both chromium species, and two of them (Magnetite and Hausmannite) reduced the hazardous Cr(VI) to Cr(III) determined by X-ray absorption spectroscopy. The materials were effective at removing both chromium ions from solution ns containing competing anions.

Table of Contents **Page**

List of Tables

List of Figures

1. Introduction

1.1 Chromium

Chromium is a naturally occurring metal that is found in ore. It is also a necessary trace element for mammals [1]. Chromium has a large array of ions that can be formed when it is utilized in different applications. However, only two of these ions are stable and can be found in large amounts. Hexavalent chromium (Cr(VI)) is a carcinogenic ion that is produced directly from anthropogenic sources. Anthropogenic sources of hexavalent chromium originated from the electroplating industry, paint pigments, and leather tanning [2,3]. Hexavalent chromium occurs in nature as an oxoanion CrO_4^{2-}, and does not occur as a typical cation [3]. Chromium is often utilized as a coating on more reactive metals in order to prevent oxidation reaction from occurring, thus making metal more durable. In terms of pigments, chromite ore is mined then processed, yielding vibrant colored salts used for both the pigments and chrome plating [2,3]. Inhalation of hexavalent chromium leads to the development of lung cancer, which is a substantial problem for metal workers in the chrome plating industry [1]. Skin absorption is another form of chromium poisoning; at low levels it can leave ulcerations [3].

The other stable chromium ion is the trivalent cation, which contrary to the hexavalent variant is found in nature. Trivalent chromium is an essential nutrient that is necessary for different biological function such as receptor binding in insulin, glucose, lipid and protein metabolism [1,4]. In the leather tanning industry, trivalent salts such as Cr(III) sulfate are used to stabilize the cross linkage between the collagen fibers found inside the pelts, which creates leather [4].

There are several ways that Cr(VI) can enter the environment; Cr(VI) can be found in the atmosphere, water sources and soil [5]. One way is through airborne introduction, which is observed in electroplating and the paint pigment industries. Another possible way of introducing chromium is through runoff from rain that comes into contact with contaminated soil that is found at chromite processing or leather tannery sites [5]. In terms of which industry releases these ions; electroplating tends to release trivalent chromium, while paint industry and the leather tanning industry release the hexavalent ion [6]. The United States is not one of the leading producers of chromite ore, but it is one of the leading manufacturers of chromium products needed for tanning, pigments, and electroplating etc [7].

1.2 Chromium poisoning

Chromium poisoning is an extremely serious issue. Currently, the EPA has established regulations on how much chromium can be introduced into the environment [8]. The current allowed concentration for hexavalent chromium is 0.100 ppm [8]. Trivalent chromium causes mutation to DNA, since its affinity to bind to DNA is higher than other species of chromium [1]. Ironically, the trivalent species cannot pass through the cell membrane, thus making any contact with trivalent chromium relatively harmless. Cr(III) is harmless due to the fact that it is incompatible with the sulfate transport mechanism, which is the system that introduces the chromium to the inner compartments of the cell [1]. On the other hand the chromate ion is compatible with the sulfate transport system [9]. Upon entering the cell, the chromate ion can undergo different reduction pathways. Once the Cr(VI) enters the cellular membrane it undergoes a reduction reaction to a Cr(V) species for a short time. Then the Cr(V) is further reduced to form Cr(IV) species and finally the chromium is reduced to Cr(III) species. The

reduction process can be initiated by the introduction of a reducing agent such as ascorbic acid or low molecular weight thoils (e.g. reduced glutathione or cystein and in some cases peroxides). The reducing agent determines the number of steps required for the reduction process [1,10]. When either peroxides or ascorbic acid are used in the reduction process hydroxyl species are generated. These damage DNA strands and can result in apoptosis of some cells [10]. As mentioned earlier ingestion of chromium is a common means of exposure to chromium ions and particularly through drinking water.

The different processes' that are involved in making these products expose many workers to the dangerously high amounts of chromium which could lead to chromium poisoning [1]. Workers numbering in the hundreds of thousands in the chrome plating, paint pigment, wood preservation, and leather tanning industries are exposed to large amounts of hexavalent compounds; furthermore, many of these exposed workers develop lung cancer due to inhalation of the hexavalent compounds [1].

1.3 Oxide materials as a method of removal

Iron oxide materials, such as Magnetite (Fe_3O_4) and similar oxide materials, have been known to sequester Cr(VI) [11-12]. One study utilized Magnetite with coatings of biogenetic amorphous silica known as diatomite [11]. The diatomite study mentioned binding capacities of 69.2 and 21.7 mg/g for the coated and non-coated material, respectively. Yuan et al. stated that the diatomite supported material was better dispersed and was able to have a larger surface area compared to the none-supported materials, thus allowing more binding sites for the two chromium ions [11]. Additionally, Yuan et al. [11] reported that one of their discoveries and possibly the most important one of all was the ability of the Magnetite material to reduce the hazardous Cr(VI) to the much safer Cr(III). Another study introduced a similar nanomaterial

known as Jacobsite ($MnFe_2O_4$). The authors reported that at pH 2 the capacity of the Jacobsite was 31.55 mg/g, they proposed that at lower pH levels, the excess hydrogen ions bind to the surface of the Jacobsite, thus making the surface cationic which the oxoanion (chromate) can easily bind to [12]. The same can be said about the Magnetite at the low pH levels that were used in the experiments. To our knowledge there are no articles concerning the sequestering of chromium by Hausmannite (Mn_3O_4) from water.

1.4 Reduction mechanism between oxide materials and chromium

Magnetite (Fe_3O_4) essentially has a chemical makeup of two octahedral oriented Fe(III) atoms bound to oxygen species, and a tetrahedral-oriented Fe(II) atom. Researchers that have studied Magnetite have reported that upon contact with the Magnetite, Cr(VI) is reduced to Cr(III) [13]. The researchers also reported that upon the binding of the Cr(VI) oxoanion to the Magnetite, one of the iron atoms caused the reduction concluding that the Fe(II) in the center of the Magnetite transferred electrons to the Cr(VI) and effectively reducing it to Cr(III) [13]. Some studies have shown that upon transferring electrons to the Cr(VI), the Magnetite transforms into maghemite (γ-Fe_2O_3) [11]. Other studies have shown that the chromate and the Magnetite form a compound that is similar to the structure found in the chromite ore [14]. Jacobsite ($MnFe_2O_4$), which has the same crystal structure as Magnetite has also been tested for sequestering Cr(VI). This material contains two Fe(III) atoms that have an octahedral orientation and at the center is a Mn(II) atom with a tetrahedral orientation that should behave like the Fe(II) found at the center of the Magnetite nanomaterial. The authors reported that the Jacobsite, like Magnetite, showed an affinity for Cr(VI) but it did not reduce the toxic Cr(VI) to the harmless Cr(III). Hu et al. [12] suggested that the bonding between the oxoanionic chromate and the nano-Jacobsite is relatively weak when compared to the bonding between the chromate and

nano-Magnetite. Hausmannite contains a Mn(II) site, which like Magnetite, is located in the center of the material, which suggests that if Cr(VI) were to bind to the Hausmannite material, it to would reduce the Cr(VI) to Cr(III) in the same fashion as the Magnetite.

1.5 Similar studies

Currently there are several methods in chromium remediation (most at low pH levels); including adsorption to ion exchange; but the most widely used technique for chromium removal is adsorption using natural minerals to fully synthetic organic compounds [11,15]. Some examples of these materials are MCM-41 and MCM-48, which are synthetic mesoporous materials, which displayed a binding (adsorption) to chromium, of 128.2 and 153.8 mg/g, respectively [15]. Anbia et al. [15] reported that at a pH level between 2 and 3 the entire surface of the mesopourous material becomes cationic in nature. This cationic nature is a result of excess protons due to a low pH. The excess of hydrogen ions protonate the negatively charged sites in the material thus providing several binding sites for the negatively charged chromate anion [15]. Other studies on sequestering chromium utilize mineral oxides such as aluminum oxyhdroxide materials since these materials have an affinity for heavy metal binding [16]. Some oxide materials such as alumina materials have shown a Cr binding capacity of 2.158 mg/g. Ajouyeda et al. [16] reported that upon contact with the chromium ions the alumina underwent an ion exchange reaction between the hydroxide functional groups found on the surface of the alumina material and the chromate contaminant. Some of the current methods utilized by the EPA are ion exchange, reverse osmosis, lime softening, and coagulation/filtration [17]. These methods, while somewhat affective, prove to be costly, non-renewable or produce large amounts of waste.

1.6 Objectives

The general objective of this study was to determine the binding capacity of Magnetite, Jacobsite and Hausmannite nanomaterials to Cr(III) and Cr(VI) synthesized using two different techniques. One of the techniques was the "closed" micro-waved synthesis and the other was the "open" (heating mantle) synthesis materials. The specific objectives were: 1) do determine at what pH the two chromium ions bind to the different materials, 2) to determine the amount of time necessary for significant amounts of the chromium to bind to the materials, 3) to determine the chromium binding capacities of the nanomaterials, and 4) to determine the binding of the two chromium ions in solutions that contain various amounts of competing anions (e.g. Cl^-, NO_3^-, SO_4^{2-} and PO_4^{3-}).

1.7 Hypotheses

This investigation was performed under the working hypotheses that 1) the two chromium would bind to the "closed"/"open" nano Magnetite and Hausmannite and the "closed" Jacobsite, 2) The Cr(VI) ion will reduce to Cr(III) upon binding to the different nanomaterials, 3) The nanomaterials would be able to sequester the majority of the chromium from the interference experiment regardless of the concentration of competing anions.

2. Sorption of Cr(III) and Cr(VI) to High and Low Pressure Synthetic Nano-Magnetite (Fe_3O_4)Particles

Abstract

Chromium exists in the environment in two common oxidation states (other than Cr(0)), which are Cr(III) and Cr(VI). These two oxidation states have very different health effects in living organisms. Cr(III) is relatively non-toxic to living organisms; however, Cr(VI) is very toxic to most living organisms. In this study we have investigated the binding of Cr(III) and Cr(VI) to an engineered nanomaterial, Magnetite, synthesized using two different synthesis techniques. The synthesis were performed using a traditional synthesis technique which involved the titration of iron(II) chloride with sodium hydroxide at a molar ratio of 3 (OH) to 1 Fe(II) ion. Subsequent to the titration the samples were aged using different techniques. The first ageing technique used was a traditional heating source in an open vessel at 90ºC for 60 min. The second ageing technique was a microwave assisted hydrothermal synthesis using a closed vessel at 90ºC for 30 min. The batch binding studies showed that Cr(III) and Cr(VI) bind to the nanomaterials differently at different pHs. In addition, Cr(III) bound to both the open vessel and the hydrothermally synthesized nanoparticles showed similar binding at all pH levels. But the Cr(VI) showed differences in the binding to the open vessel and the closed vessel nano-Magnetite, with higher binding at lower pHs observed with the open vessel compared to the closed vessel nanomaterials. Further data obtained from the batch studies included time dependency, isotherm capacities and interference studies.

2.1. Introduction

Chromium, an omnipresent element, can be found in soils, rocks and living organisms [1]. It is utilized mainly in industry for its anti-corrosive properties. For example, metals that are prone to corrosion are usually coated with chromium to prevent the oxidation process [2]. Other applications include the pigment and paint industry, and leather tanning [3]. However, the different processes that are involved in making these products expose many workers to the dangerously high amounts of chromium which could lead to chromium poisoning [1]. Workers numbering in the hundreds of thousands in the chrome plating industry are exposed to large amounts of hexavalent compounds. Furthermore, many of these exposed workers develop lung cancer due to inhalation of the hexavalent chromium compounds [1]. Other known routes of exposure to chromium include ingestion and skin absorption [4]. Even at low concentrations, skin absorption of hexavalent chromium result in ulcerations on the skin [4].

In contrast to the toxicity of Cr(VI), Cr(III) is a micro nutrient necessary in the biological activity of different enzymes and hormones such as insulin [1]. However, Cr(III) species at high concentrations inside of the cell can damage DNA. For that reason, biological mechanisms prevent large concentrations of trivalent chromium from entering the cells. One example of this is the incompatibility of Cr(III) with the sulfate transport mechanism [4]. However, hexavalent chromium is toxic and carcinogenic due to the mechanism involved in its reduction to the trivalent state [4]. Once the Cr(VI) enters a cellular membrane by way of the sulfate transport mechanism, it undergoes a reduction reaction to a Cr(V). then to Cr(IV) and finally to Cr(III) [1]. The reduction process can be initiated by the introduction of a reducing agent such as ascorbic acid and low molecular weight thiols (reduced glutathione or cystein and in some cases peroxides); the reducing agent determines the number of steps required for the reduction process

[1]. When either peroxides or ascorbic acid is used in the reduction process, hydroxyl species are generated, which damage DNA strands and can result in the apoptosis of particular cells [5]. As mentioned earlier, ingestion of chromium is a common means of exposure to chromium ions, particularly through drinking water. Currently, the EPA has limited the amount of total chromium in drinking water to 0.100 ppm [6].

A possible method to remove Cr(VI) from the aqueous environment may be through the use of natural and synthetic materials, such iron oxide materials [7-28]. Iron oxide materials have been shown to adsorb both Cr(III) and Cr(VI) in aqueous solutions [7]. Furthermore, many iron oxide materials containing Fe^{2+} ions reduce Cr(VI) to Cr(III) ions by transferring electrons from the Fe(II) to the Cr(VI) [8]. Alternatively, co-precipitation of chromium with iron has also been investigated. For example, the sorption of Cr(VI) from solution has been studied using diatomite-supported and unsupported Magnetite particles at the micro and nano sizes. A high efficiency of removal and good capacities has been observed at pH of 11.4 and 10.6 for the supported and unsupported nano-Magnetite particles [8]. At the nanoscale the capacities were observed to increase to 69.2 and 21.7 mg/g for the supported and unsupported nano-magneite particles, respectively [8]. Similarly, montmorolinite-supported iron oxide nanoparticles have also shown excellent removal of Cr(VI) from aqueous solutions [9]. There are other examples in the literature that show a high affinity of Cr(III) to iron oxide materials. One advantage of using the iron oxide materials is, if the materials dissolve, it only releases iron into solution, which is an essential nutrient. Another advantage of using iron nanomaterial systems is that they show little to no interference in the binding of the chromium ions to the material, even in the presence of a high concentration of competing ions [10].

In the current study the binding of Cr(III) and Cr(VI) to nano-magentite was investigated. The nano-magentite investigated was aged under two different conditions: a traditional heating with an open vessel and a microwave-assisted heating in a closed vessel. The reaction of the nanophases and chromium solutions were carried out not only to observe the binding of the chromium from pH 2 through pH 6 but to investigate the time dependency of the binding as well. Further studies were performed using isotherms to determine the binding capacity of the materials. In addition, studies were performed to determine the effects of different anions including chloride, nitrate, sulfate, and phosphate.

2.2. Methodology

2.2.1. Synthesis of iron oxide nanoparticles

The procedure for the synthesis of the particles was similar to that reported by Parsons et al. [11]. A 30 mM solution of iron(II) chloride was prepared from iron(II) chloride tetrahydrate and deionized (DI) water. The amount of salt used was 5.96g and it was dissolved in 1.0L of DI water. The solution was then titrated with a 1M solution of sodium hydroxide. The hydroxide was added to the iron(II) solution through a slow titration at an approximate rate of 0.1mL/min using a burette. The solution was kept under constant stirring to obtain a homogenous mixture. The rate of titration was kept at a constant to help control the size of the particle. The resulting material was iron hydroxide in the form of $Fe(OH)_2$, which was then converted to Magnetite (Fe_3O_4) using heat.

2.2.2 Ageing of the nano-magnetite

The $Fe(OH)_2$ was then placed in a Teflon vessel and put into a Perkin Elmer Multiwave 2000 system. The particles were heated at a constant temperature of 90 ºC for 30 min and subsequently cooled to room temperature. The cooled samples were then centrifuged at 3000 rpm for approximately ten min and the supernatant was discarded. The particles were then dried in an oven at 100°C until completely dry. The open vessel ageing process followed the same procedure as the microwave-aged particles, but instead of microwaving the particles, they were placed on a heating mantle and heated to 90°C for 1h.

2.2.3. pH study

For the pH profile studies, two sets of 100 ppb chromium solutions were prepared, one set for the Cr(III) and one set for the Cr(VI). Cr(III) and Cr(VI) solutions were prepared from chromium nitrate and potassium dichromate salts, respectively. Solutions of both ions (100 ppb) were then pH-adjusted to 2, 3, 4, 5, and 6; this was performed by addition of small amounts of either HCl or NaOH at 0.001M level with the solutions under constant stirring [29].

Once the pH-adjusted solutions were prepared, with either the Cr(III) or Cr(VI) ions, 10 mg of the synthesized iron oxide nanoparticle were weighed and placed into a 5 mL plastic test tube in triplicate. After weighing, four milliliters of the pH-adjusted chromium solution were added to the test tubes. The test tubes were then capped and placed on a speci-mix rocker to equilibrate for 1h. In addition, controls for the reactions consisted of the chromium ions without the iron nanoparticles, in triplicate for statistical purposes. Subsequent to the reaction, the samples were centrifuged at 3000 rpm for 5min and the supernatant was collected and saved for further analysis. The control samples were treated in the same way as the reaction samples.

2.2.4. Time dependency study

The chromium solutions, either Cr(III) or Cr(VI) were pH-adjusted to the optimum pH level using either dilute hydrochloric acid or dilute sodium hydroxide. Again, 10 mg of the nano-Magnetite were weighed out and placed in to a 5 mL plastic test tube and 4 mL of the pH-adjusted Cr(III) or Cr(VI) ions were added to the test tube. Subsequent to the addition of the chromium ion solution, the samples were capped and placed on a rocker to equilibrate for times of 5, 10, 15, 20, 30, and 60 min. Again, controls for the reactions consisted of the chromium solution without the nano-Magnetite. These reactions were performed in triplicate. Subsequent to the reaction, the samples were centrifuged at 3000 rpm for 5 min and the supernatant was collected and saved for further analysis. The control samples were treated in the same way as the reaction samples.

2.2.5. Adsorption isotherm

This study was performed under a similar procedure as the pH study, but at a fixed reaction time of 1.0 h. The solution concentrations for each of the chromium species used in this study were 10, 5, 1, 0.5, and 0.25 ppm. A 10 mg sample of the nano-Magnetite was weighed out and placed into a 5.0 mL plastic test tube. This was performed in triplicate. A 4.0 mL aliquot of one of the pH-adjusted chromium solutions was added to the nano-Magnetite sample, in the test tube. The sample and the chromium solution were then capped and placed on a rocker to equilibrate for 1 h. Again, controls for the reactions consisted of the chromium solution without the nano-Magnetite. These reactions were performed in triplicate for statistical purposes. Subsequent to the reaction, the samples were centrifuged at 3000 rpm for 5 min and the supernatant was collected and saved for further analysis.

2.2.6. Interference study

This study was performed in a similar manner as the isotherm studies with the exception that interfering ions were added to the reaction solutions. The interfering anions used for this study were phosphate, sulfate, chloride, and nitrate, which were obtained from their sodium salts. Solutions contacting 100 ppb of either Cr(III) or Cr(VI) were prepared containing 0.1, 1.0, 10, 100 ppm of the anions. The solutions were subsequently pH-adjusted to pH 4 as previously mentioned. A 10 mg sample of the nano-Magnetite was weighed out and placed in a 5 mL test tube. Then a 4.0 mL aliquot of one of the pH-adjusted chromium solutions contacting one of the anions was added to the nano-Magnetite sample, while in the test tube. The sample and the chromium solution was then capped and placed on a rocker to equilibrate for 1 h. Controls for the reactions consisted of the chromium solution without the nano-Magnetite. These reactions were performed in triplicate. Subsequent to the reaction, the samples were centrifuged at 3000 rpm for 5 min and the supernatant was collected and saved for further analysis. The procedure was repeated for each of the chromium ions that were mixed with each of the interfering ions.

2.2.7. GFAAS

A Perkin Elmer® Zeeman graphite furnace atomic absorption spectrometer model 5100ZL (Perkin Elmer-Shelton, CT) was used to determine the chromium concentration in solution. The calibration of the instrument was performed using a set of chromium standards prepared using a chromium standard purchased from PlasmaCAL®. Concentrations of 10, 50, and 100 ppb were made from serial dilutions of a 1000 ppm stock solution. A matrix modifier consisting of .015 mg of $Mg(NO_3)_2$ was used for the analysis. The lamp current for the Cr lamp was 25 mA, with a wavelength of 350 nm and the slit size being 0.7 mm. These conditions were

used for all analysis. In addition, all calibration curves obtained had a R^2 value of at least 0.99 or better.

2.2.9 Statistical analysis

The triplicate data of the chromium solutions were analyzed with one-way analysis of variance using SPSS software, version 17.0 (SPSS Inc., Chicago, IL). Significant differences were detected using the Tukey-HSD (honestly significant difference) test. Any reference to a significant difference between data is based on a probability of $p < 0.05$, unless otherwise stated.

2.2.8 X-ray diffraction analysis

The characterization of the synthesized Fe_3O_4 nanomaterial was performed via powder X-ray diffraction using a Bruker AXS GmbH (Germany). The samples were first homogenized with a mortar and pestle and placed on to a platinum sample holder. The samples were diffracted from 20-60° in 2θ using an 8s counting time and a stepping rate of 0.007°/min at room temperature. Using crystallographic data from the literature, as well as nj[j], fittings were conducted. A Le Bail fitting was performed in FullProf to determine the phase of the material. In addition, the size of the nanoparticles was determined using Scherrer's equation and a Gaussian fitting of the data was used as well, with an average of three different diffraction peaks in the sample.

2.3 Results and Discussion

2.3.1 XRD characterization results

Figure 2.1 shows the diffraction pattern of the synthesized nanomaterials under the open vessel conditions and the microwave-assisted synthesized nanomaterial. As can be seen in Figure 1, the nanomaterials had the 220, 311, 400, 422, and 333 planes in the material, showing

that the materials both have the structure of Magnetite [30]. Also it should be noted that the sample's holder was platinum and the 111 and the 220 diffraction peaks are clearly visible in the diffraction pattern as displayed in Figure 1. In addition, using the Scherrer's equation, the average size of the nanomaterials was found to be 27 nm for the open vessel synthesis. The size of the microwave-assisted Fe_3O_4 nanomaterials was 25 nm. As mentioned in the experimental section, the size was determined based on three different diffraction peaks. These particles were then used in the various different studies in this investigation.

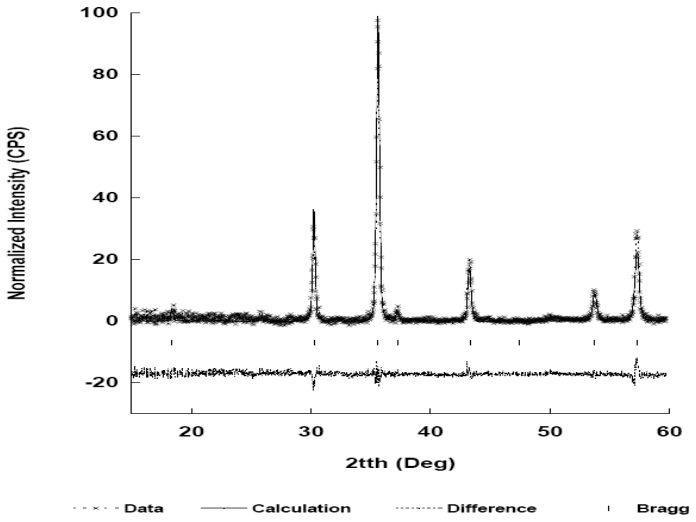

Figure 2.1 Diffraction pattern for Magnetite

2.3.2 pH dependency

Figure 2.2 and 2.3 show the adsorption of Cr(VI) and Cr(III) to the synthesized nano-Magnetite using an open vessel synthesis and the microwave-assisted synthesis. As can be seen in Figure 2, Cr(VI) was pH dependent in its binding to both the Fe_3O_4 nanomaterials , at lower levels there was some statistical difference between pH 2 and 3 but showed low binding. In addition, the binding for the Cr(VI) becomes maximized around pH 4 and remained relatively

constant thereafter with the microwave-assisted, synthesized Fe_3O_4 with no statistical difference at pH 5 and 6. However, the binding of the Cr(VI) anions to the open vessel Fe_3O_4 nanomaterial maximizes at pH 4 and then decreased at pH 5 and pH 6 were the binding showed a significant difference from the other pH levels. Cr(III) binding did not occur at pH 2, and very minimal binding was observed at pH 3 which. However, the binding increases to approximately 95-100% at pH 4 for both Fe_3O_4 nanomaterials. Once the binding of the nanomaterials maximized at pH 4, it remained relatively constant thereafter. Statistically different only a pH levels below 4 for both materials. These types of binding trends have been observed for the binding of Cr(III) and Cr(VI) to iron nanomaterials [12,13]. For example, the percentage removal of Cr(VI) using supported/unsupported diatomite showed approximately 100% of the Cr(VI) [8], whereas micro-sized Magnetite particles bond approximately 50% of the chromium from solution. The binding of the Cr(VI) was stable at a low pH from 1-3 and decreased with increasing pH up to pH 8 [8]. In a similar study using Montmorillonite-supported Magnetite nanoparticles, the authors observed high binding of Cr(VI) at a low pH and decreased binding above pH 3. In the current study the results of the Magnetite that was synthesized using the open vessel technique followed a similar trend. However, the nano-Magnetite that was synthesized using the microwave-assisted synthesis did not show the decrease in the binding even at pH 6. This difference in the binding of the Cr(VI) to the open vessel and the closed vessel may be due to the ageing process. The microwave-assisted synthesized Fe_3O_4, aged in a closed vessel, was limited in the amount of oxygen and could provide more Fe^{2+} or some un-reacted OH^- groups on the surface; whereas the ageing of the nanomaterials in the open vessel were exposed to an excess of oxygen which may have lead to the formation of a layer of Fe^{3+} which would enhance the binding of Cr(VI) to these materials.

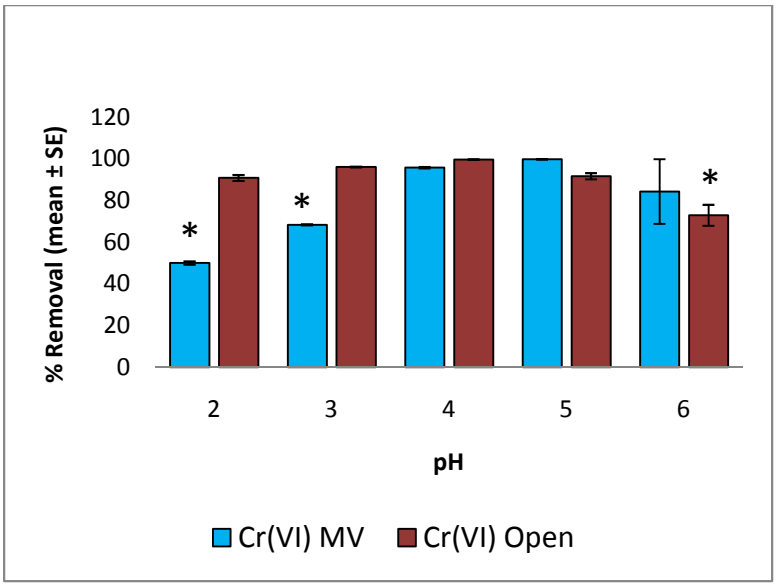

Figure 2.2 Sorption of Cr(VI) to open and closed system synthesized nano-Magnetite at pH 2-6. The error bars represent ± standard error. * indicate statistical differences ($p<0.05$). Comparisons were made within the microwave material (MV) and open (non-microwave) material.

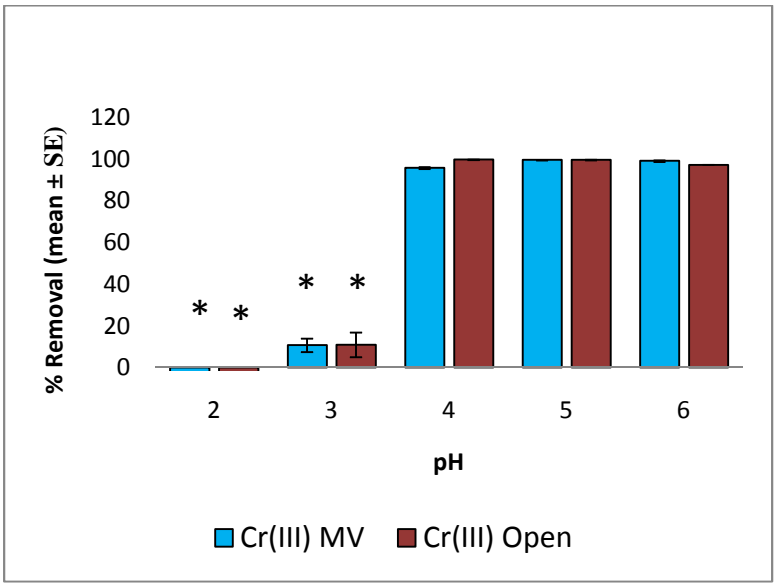

Figure 2.3 Sorption of Cr(III) to open and closed system synthesized nano-Magnetite at pH 2-6. The error bars represent ± standard error. * indicate statistical differences ($p<0.05$). Comparisons were made within the microwave material (MV) and open (non-microwave) material.

The sorption of chromate to $Fe_2O_3H_2O$ has also been shown to be pH dependent with approximately 100% binding of a 5.0 x10^{-6} M solution of CrO_4^{2-} or approximately 0.0005 ppm of chromium.The binding was found to reduce above pH 6 and reach a binding of 0% between pH 8 and pH 10 under different reaction conditions [14]. This deviation in the binding at pH 5 and pH 6 of the microwave-assisted, synthesized nanoparticles may be due to the formation of a surface layer of FeOOH, which is supported in the results and the literature.

2.3.2 Time dependency studies

Figure 2.4 and 2.5 show the time dependency of the binding of both Cr(III) and Cr(VI) to the open vessel and microwave-assisted, synthesized Fe_3O_4 nanomaterials. The Cr(VI) bound rapidly to the microwave-assisted, synthesized nano-Magnetite, which occurred within the first 5 min and remained constant after 1 h of time. The Cr(III) reacted with the microwave-assisted synthesized Fe_3O_4 showed a slight increase in binding as contact time increased, after 15 min the binding remained constant. The Cr(VI) binding occurred at approximately 70% and remained constant for the first 30 min and then increased up to 95 to 100 %. Whereas the binding of the Cr(III) to the open vessel nanoparticles showed very low binding in the time ranging from 5 min to 30 min, the binding, by the 1h mark, maximized to above 90%. The binding of the Cr(VI) to the open vessel synthesized Fe_3O_4 showed a relatively constant binding up to 30 min with a slight increase in the binding from 70% to approximately 90% between 30 and 60 min of contact time. Similarly in the literature, the time dependency of chromium binding to nanomaterials has been shown [15]. However, Cr(VI) generally requires more time to bind than Cr(III) due to different redox reactions and chemical kinetics occurring in the reaction [15]

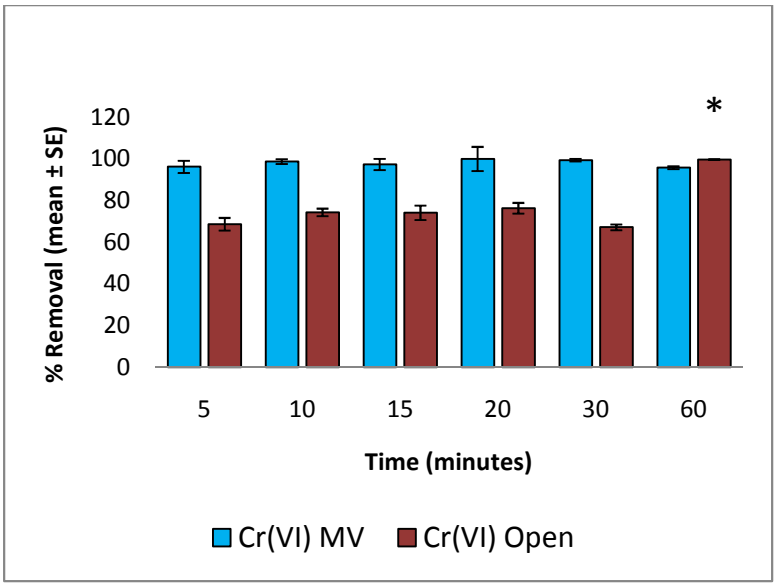

Figure 2.4 Time dependence of Cr(VI) adsorption at a concentration of 100ppb and pH 4 to open and closed system Magnetite. Error bars represent ± standard error. * indicates statistical differences ($p<0.05$). Comparisons were made within the microwave material (MV) and open (non-microwave) material.

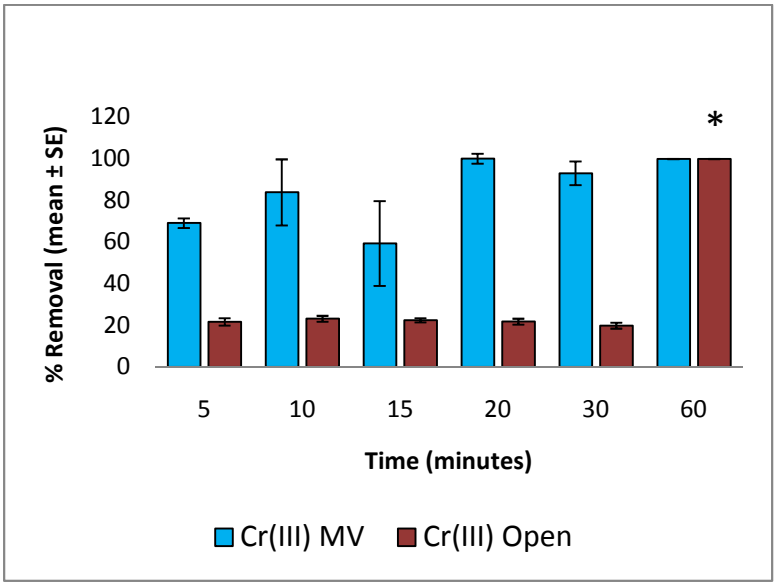

Figure 2.5 Time dependence of Cr(III) adsorption at a concentration of 100ppb and pH 4 to open and closed system Magnetite. Error bars represent ± standard error. * indicates statistical differences ($p<0.05$). Comparisons were made within the microwave material (MV) and open (non-microwave) material.

The binding in the two different studies showed no difference statistically from the 5-30 min range. The 1 h mark is the only area that should a statistical difference throughout the different treatments.

2.3.3 Adsorption isotherms

In this study adsorption isotherms were used to determine the capacities of the microwave-synthesized and the open vessel-synthesized nano-Magnetite. The isotherms were fitted using the Langmuir isotherm equation as shown below in the linearized format:

$$\frac{C_e}{Q_e} = \frac{1}{(bQ_m)} + \frac{1}{(Q_m)} C_e$$

Where C_e is the equilibrium concentration of the Cr(VI) in solution, b is a constant that is related to the ionic strength and the pH of the solution. Q_m is the capacity of the material. The capacities determined using the Langmuir equation are shown in Table 2.1.

Table 2.1 Cr(VI) and Cr(III) binding capacities based on different solution concentrations to both open and closed system nanophases

Sample	Capacity (mg/kg)	SE (+/- mg/kg)
Fe_3O_4 Cr(VI) MV	1208	43.9
Fe_3O_4 Cr(VI) Op	1705	14.5
Fe_3O_4 Cr(III) MV	555	10.5
Fe_3O_4 Cr(III) Op	555	2.2

This current study showed binding capacities of 555 ± 2.2 mg/kg and 1705 ± 14.5 mg/kg (or 0.5 mg/g and 1.705 mg/g) to Cr(III) and Cr(VI) for the open vessel synthesized Fe_3O_4 nanomaterial. Similar values of 555 ± 10.5 and 1208 ± 43.9 were obtained in the reaction of Cr(III) and Cr(VI) to the microwave synthesized Fe_3O_4 nanomaterial respectively. Smith and Ghiassi found a capacity of 9.5 +/- 0.3 mg/g for the binding of chromate to iron(III) oxyhydroxide [16]. Smith and Ghiassi [16] also noted that there was some co-precipitation occurring in the reactions through the dissolution of Fe(II) and the formation of Cr(III)- iron complex. The high capacity of the iron(III) oxyhydroxide materials is not only through the sorption of the chromium but also a co-precipitation. Yun Peng et al. [8] have investigated the removal of Cr(VI) from aqueous solutions by diatomite-supported and -unsupported magnetic nanoparticles. The researchers found that the diatomite-supported nanoparticles showed higher capacities than the unsupported nanoparticles. The observed capacities of the supported and unsupported microscale particles for the Cr(VI) were 11.4 mg/g and 10.6 mg/g, respectively; however, the nanoscale Magnetite capacities of 69.2 and 21.7 mg/g were observed for the supported and unsupported nanoparticles. The increase in the capacities of the nanomaterials, when supported, indicates that the diatomite has a high capacity for binding Cr(VI) from aqueous solution possibly due to the surface modification by the diatomite clay, which has been shown to be 11.55 mg/g [8]. A similar material, γ-Fe_2O_3 in the nanophase, has been studied for the removal of Cr(VI) from aqueous solutions at pH 2.5 [17]. The observed capacity of the γ-Fe_2O_3 nanoparticles was 15.6 mg/g. For Anatase, another iron based material, the capacity for Cr(VI) has been observed to be 14.56 mg/g [20]. Other systems have been investigated for the removal of Cr(VI) from aqueous solutions, such as aluminum/magnesium-mixed hydroxides which have shown capacities in the range of 105.3 to112.0 mg/g [18]. The literature shows that Fe_2O_3 has a

higher binding capacity than the Fe_3O_4 materials, as does FeOOH, another iron(III) compound. The preparation of nanomaterials controls their reactivity and the functionality [19]. In addition, some of the studies that show long equilibrium time and low pH's result in high chromium binding [8,9,12,13,]. In a study by Parsons et al [29], the adsorption of As(III) and As(V) was studied using different nanomaterials including Fe_3O_4. This study showed that at low pH the iron-based nanomaterials released large amounts of iron which decreased only by increasing the pH up to pH 6 [29]. The data indicates that the high capacity observed for the binding of iron oxide nanomaterials could potentially be a co-precipitation reaction as mentioned by Smith and Ghiassi [16]. The lower capacities in the current studies may be due to the pH of the solution and the amount of dissolved iron in the solution.

2.3.4 Interference studies

Figures 2.6-2.9 show the effects that common anions (Cl^-, NO_3^-, SO_4^{2-}, and PO_4^{3-}) have on the binding of Cr(VI) and Cr(III) to the open vessel and microwave-assisted, synthesized nanomaterials at pH 4. The concentrations of interfering anions investigated were in the concentration range from 0.1 ppm to 100 ppm. As can be seen in Figures 2.6 A and B the interference studies with Cl^- anions initially showed a small decrease in binding (approximately 10%) for the reaction between the Cr(VI) and the open vessel synthesized Magnetite. A 30% decrease in the binding of the Cr(VI) to the microwave-synthesized Magnetite was also seen. The microwaved Magnetite showed an initial decrease at the lower concentrations of Cl^- and the binding remains relatively constant thereafter with statistical differences found at 1 and 100 ppm of chloride ion.

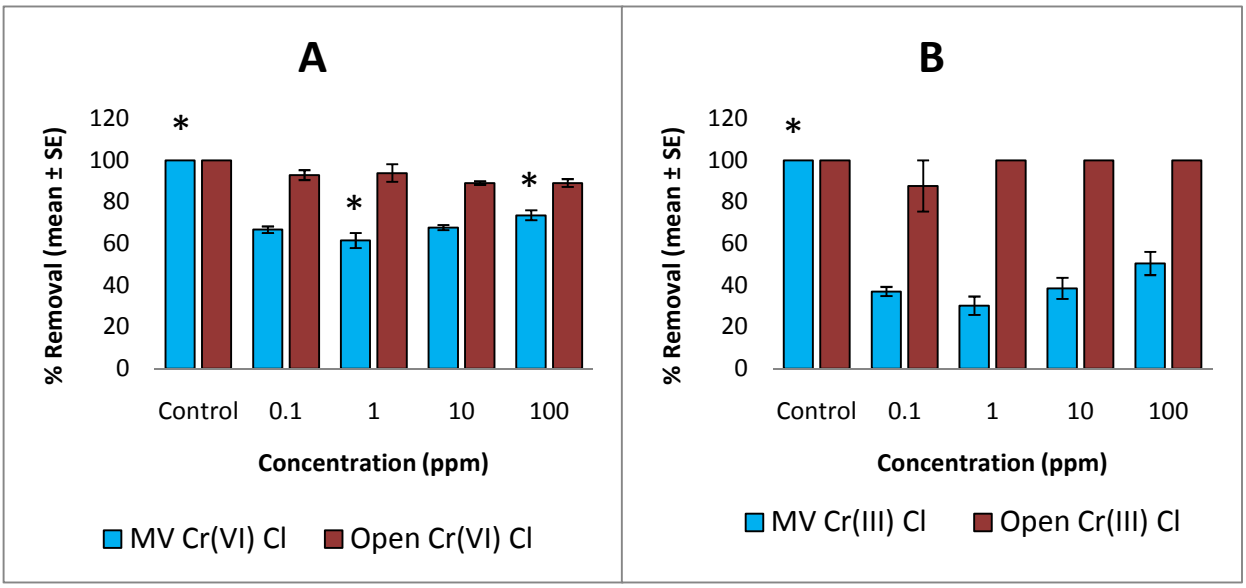

Fig 2.6. Sorption of: A. Cr(VI) and B. Cr(III) at 100 ppb to the Magnetite nanophase at different concentrations of chlorine anion. Error bars represent ± standard error. * indicates statistical differences ($p<0.05$). Comparisons were made within the microwave material (MV) and open (non-microwave) material.

Similar to the Cl^- study, the nitrate showed an initial decrease in the binding of approximately 10% and 20% for Cr(VI) binding to open and microwave-synthesized nanoparticles of Fe_3O_4 (Figures 2.7A and B). The binding of Cr(VI) to the microwave-synthesized Magnetite remained constant at around 70 % with no statistical differences except the control. The open vessel magnetite showed binding around 90% with statistical differences at 0.1 and 100 ppm aside from the control. Similar results seen in the Cr(VI) and nitrate experiments with the nitrate anions were observed for the Cr(III) experiments with statistical differences at 100 ppm for the microwave material . Low binding was observed on the binding of Cr(VI) to the nano-Magnetite in the presence of phosphate and sulfate anions which can be seen in Figures 2.8 and 2.9. However, at concentrations of 10 to 100 ppm of the interfering ions, interference in the binding was not observed. Also in the presence of the SO_4^{2-} and PO_4^{3-} a u-shaped curve was observed

with a decrease in the binding at low concentrations of SO_4^{2-} and PO_4^{3-}as seen in Figures 2.8 and 2.9. Statistical differences for 0.1 and 1 ppm sulfate solutions were seen for both the open and the microwaved synthesized Magnetite. The same statistical difference was seen for the microwaved synthesized Magnetite and the phosphate spiked Cr(VI) solution.

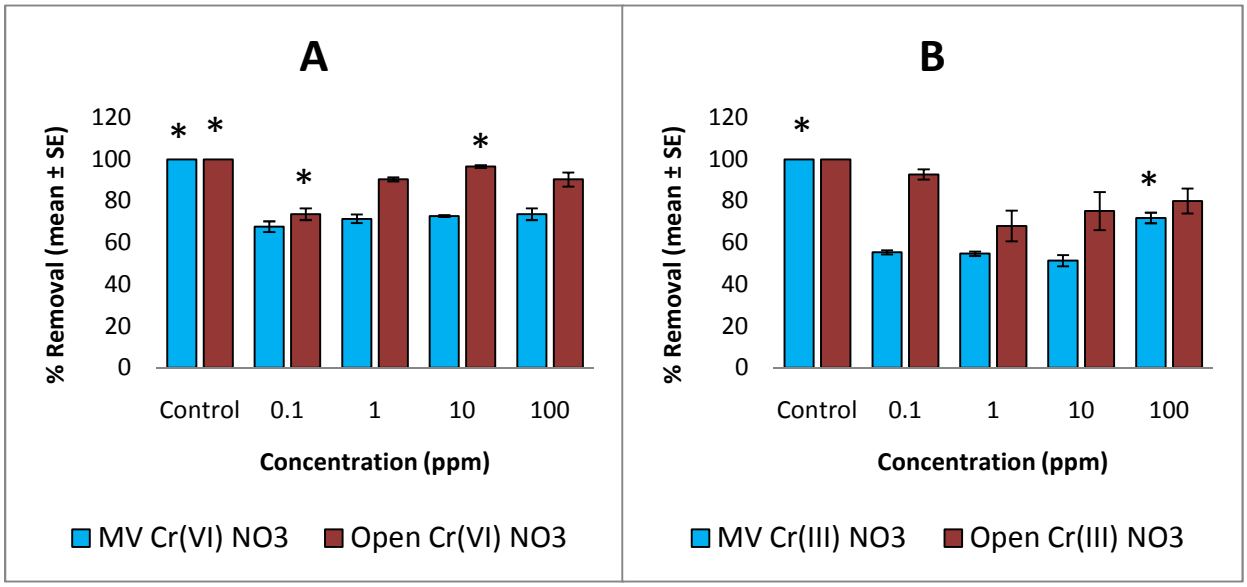

Fig 2.7. Sorption of: A. Cr(VI) and B. Cr(III) at 100 ppb to the Magnetite nanophase at different concentrations of nitrate anion. Error bars represent ± standard error. * indicates statistical differences ($p<0.05$). Comparisons were made within the microwave material (MV) and open (non-microwave) material.

The Cr(III) experiment showed the same trend as the Cr(VI) experiment but at much lower binding with an increase of binding seen at higher concentrations of interference anion. A statistical difference in the Cr(III) experiment with the sulfate ion was seen at 0.1 and 1 ppm concentrations for both the microwave and open synthesis Magnetite. The statistical difference was seen in the 0.1 and 10 ppm concentrations of phosphate that reacted with the open synthesis Magnetite and also at the 10 ppm concentration phosphate that reacted with the microwaved

Magnetite. Similar results are shown in the literature: anions such as chloride and fluoride have little to no effect on the binding of chromate to different ion oxides[19]. The adsorption of Cr(VI) in the presence of both SO_4^{2-} and PO_4^{3-} have been shown to reduce the binding [20]. However, in the study of iron-coated materials for the sorption of Cr(III) and Cr(VI) a decrease in the sorption was observed in the pH range of 3-4 [24]. Additionally, the binding does not decrease below 50% which indicates that there is some preferential binding of the chromium to the nanomaterials compared to the interfering anions. Preferential binding is observed considering that a mass ratio of chromium to the anions was1:1000. The u-shaped curves in the presence of SO_4^{2-} and PO_4^{3-} may be due to the potential modification of the surface by these anions, which may oxidize the surface of the sorbents.

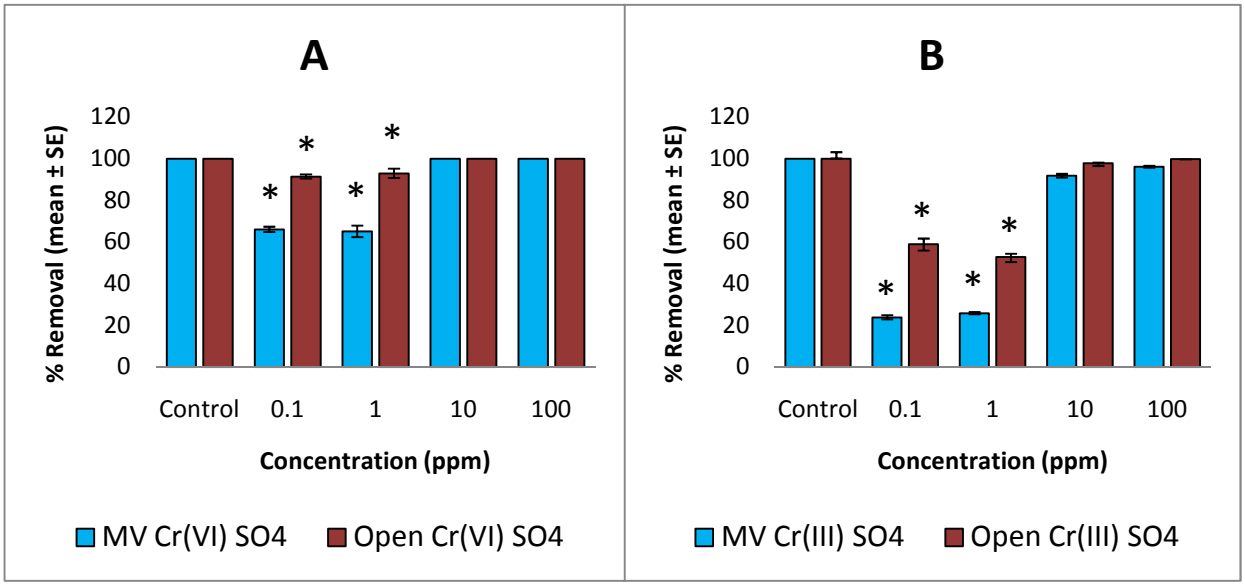

Fig 2.8. Sorption of: A. Cr(VI) and B. Cr(III) at 100ppb to the Magnetite nanophase at different concentrations of sulfate anion. Error bars represent ± standard error. * indicates statistical differences ($p<0.05$). Comparisons were made within the microwave material (MV) and open (non-microwave) material.

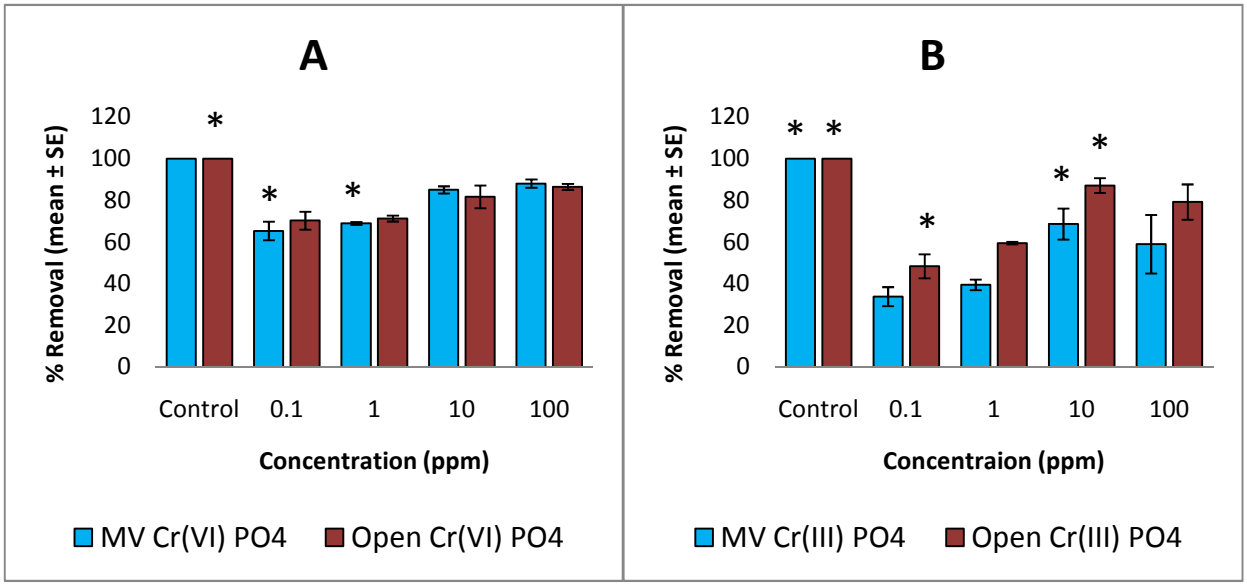

Fig 2.9. Sorption of (A) Cr(VI) and (B) Cr(III) at 100ppb to the Magnetite nanophase at different concentrations of phosphate anion. Error bars represent ± standard error. * indicates statistical differences ($p<0.05$). Comparisons were made within the microwave material (MV) and open (non-microwave) material.

2.4. Conclusion

The overall results are promising for the removal of low concentrations of both the harmful hexavalent chromium and the relatively harmless trivalent chromium from surface water. The relatively inexpensive synthesis stands out more than the microwaved system in terms of sequestering both species of chromium. The phenomenon that truly stands out is the fact that the inexpensive mineral transforms the chromium from a very harmful oxidation state to a more harmless state.

The particles showed promising results when reacted with the competing anions, the smaller charged anions showed no interference while the larger anions proved to be a bit more challenging for the particles. The anions used in this study are just a preliminary study on how the particles react to real world conditions. These anions are commonly found in surface waters

thanks to fertilizers used for soil near surface waters. Currently the only explanation as to why the bigger anions proved to be a tougher competitor could be that the ions are causing surface modification on the material. Overall the materials superseded our expectations in terms of sequestering hexavalent chromium. Further studies need to be conducted for more realistic large-scale scenarios in order to fully understand the phenomenon.

3. Sorption of Cr(III) and Cr(VI) to nano-Jacobsite ($MnFe_2O_4$)

Abstract

Hexavalent chromium has been generally known as very toxic to most living organisms, while trivalent chromium is known as a nutrient necessary for many biological functions. In this study we have investigated the binding of Cr(III) and Cr(VI) to an engineered nanomaterial, Jacobsite. Jacobsite is a naturally occurring mineral that has a composition of $MnFe_2O_4$. The synthesis was performed using a traditional synthesis technique involving the titration of Iron(II) chloride and manganese(II) sulfate with sodium hydroxide to obtain a 1:3 ratio of M^+:OH^-. Batch binding studies showed that at different pHs different amounts of the two chromium species bind to Jacobsite. The binding of both chromium species was found to be at pH 4. At this pH Jacobsite removed 70% of Cr(VI) from solution while only removing 40% of Cr(III). The necessary time required for Jacobsite to effectively bind to both species of chromium was 1h. Jacobsite showed binding capacities of 1250 (mg/kg) for Cr(VI) and 370.3 (mg/kg) for Cr(III). Additionally an interference study was performed to see how the binding trend differed by subjecting the Jacobsite to chromium solutions that contained competing anions such as Cl^-, NO_3^-, SO_4^{2-}, PO_4^{3-}.

3.1. Introduction

Different studies show that iron nanomaterials have an affinity for sequestering hexavalent chromium [1-5]. Recently there have been studies on sequestering hexavalent chromium using Jacobsite, an iron oxide material that replaces an iron for manganese. These studies have been conducted using different parameters such as pH and different time dependencies. For example, one study was conducted using Jacobsite particles sized at 10 nm and the maximum amount of hexavalent chromium they sequestered was 31.55 mg/g at pH 3 [6]. There are other materials in use to sequester chromium, such as MCM-41 and MCM-48 which are synthetic mesoporous materials that showed a binding trend of 128.2 and 153.8 mg/g, respectively [7]. Iron-manganese materials have been well-known sequestering materials for other carcinogenic anions such as arsenic [8]. Perhaps the largest advantage of using the iron-manganese oxide materials is that when dissolved iron and manganese are released into solution in miniscule amounts. One additional advantage of using the Jacobsite nanomaterial is that they show limited or no interference in the binding of the chromium ions to the material, even in the presence of high concentration of competing ions [9].

The current study will show the adsorption trends of both species of chromium with Jacobsite nanoparticles. The reaction of the nanophases and chromium solutions were performed from pH 2 through pH 6; to investigate the time necessary for the chromium to bind to the nanomaterial. Further studies were performed using isotherms to determine the binding capacity of the materials. Another set of tests were performed that involved spiking the chromium solutions with chloride, nitrate, sulfate, and phosphate will be performed, and this will help illustrate the competition between both species of chromium and the anions in order to give a real world scenario. A graphite furnace atomic adsorption spectrometer was used to determine

how much chromium was removed and an X-ray diffractometer was used to determine the size of the materials.

3.2. Methodology

3.2.1. Synthesis of manganese-iron oxide nanoparticles

The synthesis of the Jacobsite nanoparticles was described in the previous chapter. A 30 mM solution of iron(II) chloride and manganese sulfate was prepared from iron(II) chloride tetrahydrate and manganese sulfate dionized water, at 20 mM and 10 mM concentrations, respectively. The solution was then titrated with a 1M solution of sodium hydroxide. Unlike in the previous chapter, the particles were micro-waved aged using the same technique as the one used in chapter 2.

The same batch studies (pH, time dependency, capacity and interference studies) were performed as mentioned in the previous chapter in order to determine the sequestering properties of the Jacobsite in the same conditions mentioned in the previous chapter. Characterization studies were also performed on the newly synthesized materials in order to determine the crystal structure and other characterization properties.

3.3 Results and Discussion

3.3.1 XRD characterization results

The XRD spectra for the Jacobsite nanomaterial is shown in Figure 3.1. The figure displays peaks at 111, 220, 311, 400,422, 333, and 440, which are characteristic peaks of Jacobsite [11]. In addition, using the Scherrer's equation, the average size of the nanomaterial

was 27 nm. As mentioned in the experimental section, the size was determined based on three different diffraction peaks.

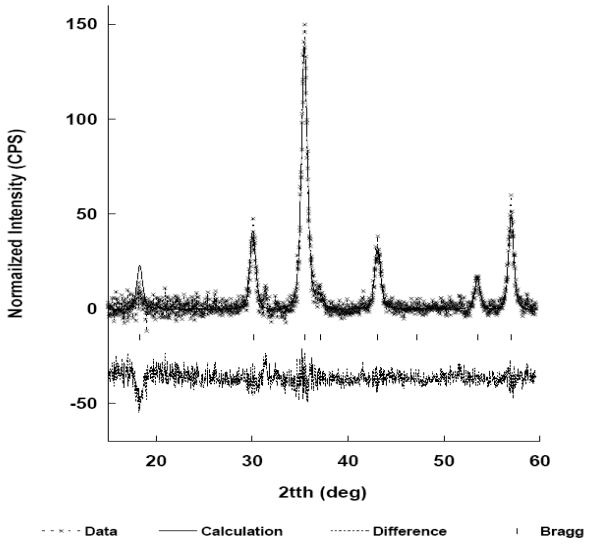

Fig 3.1 Diffraction pattern of nano-Jacobsite from 20° to 60°.

3.3.2 pH dependency

The first set of results comes from the pH profile of the experiment. Figure 3.2 illustrates the interaction of the Jacobsite nanomaterial with both of the chromium species. The binding of both chromium species to the Jacobsite nanophase was pH-dependent. Chromium binding at pH 2 was at 0% due to the fact that at more acidic conditions the particles tend to dissolve [10]. Though it would appear that the optimum pH for chromium to bind to Jacobsite seems to be around pH 6, but when comparing both ionic tests, pH 4 was the optimum pH for the Cr(VI). The statistical differences were found to be at pH level 2-3 for Cr(VI) At pH 4, the binding between Cr(VI) and Jacobsite was 70%. Cr(III) displayed the same binding trend that was seen in the Cr(VI) pH profile.

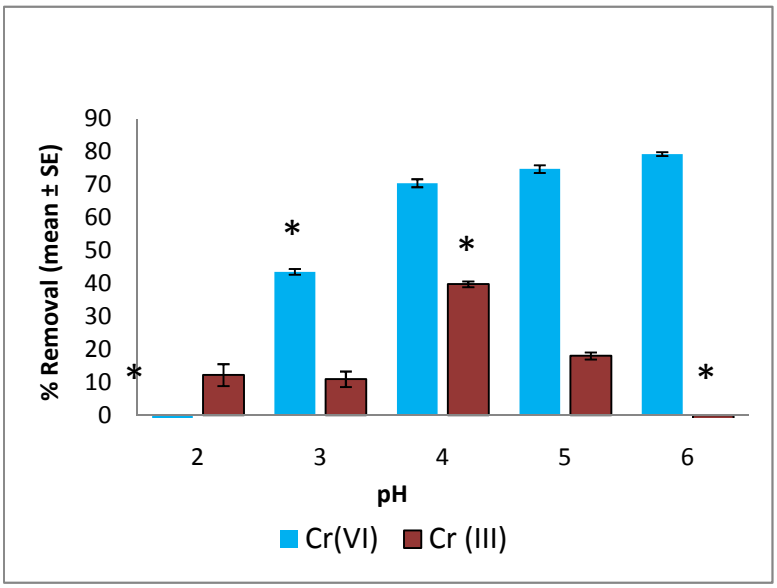

Fig.3 2. Sorption of Cr(VI) and Cr(III) under different pH conditions from pH 2-6. Error bars represent ± standard error. * indicates statistical differences ($p<0.05$). Comparisons were made within the Cr(VI) study and a separate one within the Cr(III) study.

The binding between Cr(III) and Jacobsite at pH 4 to approximately 40%. A reduction in binding was observed when the pH of the solution was increased. Statistically for Cr(III) the difference in binding occurred significantly at pH 4 and pH 6. For purposes of uniformity, the hexavalent chromium solutions were left at pH 4. Upon looking at Figure 3.2 the % removal at pH 6 was only slightly higher than the % removal at pH 4, but there was no binding for Cr(III). Similar experiments showed that the majority of the binding occurred at pH 2, such was the case in Hu et al [6]. In the experiment, the increase in pH showed a decrease in adsorption of hexavalent chromium. In a previous study concerning the binding between iron nanomaterials and Cr(VI), the binding trend between the nanomaterial and the chromium reduced above pH 6 and reach a binding of 0% between pH 8 and pH 10 under different reaction conditions [11].

This study was a deviation from that trend showing that the majority of binding occurred above pH 3.

3.3.3 Time dependency studies

The time necessary for the sequestering of both chromium species are illustrated in Fig. 3.3. For the Jacobsite nanophase that was exposed to the hexavalent chromium, it was shown that the binding at 5 min was relatively low, approximately 10%, and there was a steady increase as time increased. However, as the 1 h mark was achieved the binding jumped from 20% to 70%. Trivalent chromium showed a similar trend. Initially miniscule binding was observed in the first 5 min, remaining constant until the 15 min mark, when the binding was just above the zero mark. From there, the binding increased at 20 min to 14% but it decreased yet again to 8% after 30 min of exposure. When the nanophase and the chromium solution were exposed to each other for 60 min, the binding jumped to approximately 40%, a similar trend that occurred in the hexavalent time profile. Typically Cr(VI) generally requires more time to bind than Cr(III) due to different redox reactions and chemical kinetics occurring in the reaction [12]. The binding at the different ranges remained constant from the 5 min-30 min mark and then changed significantly at the 60 min mark for both Cr species.

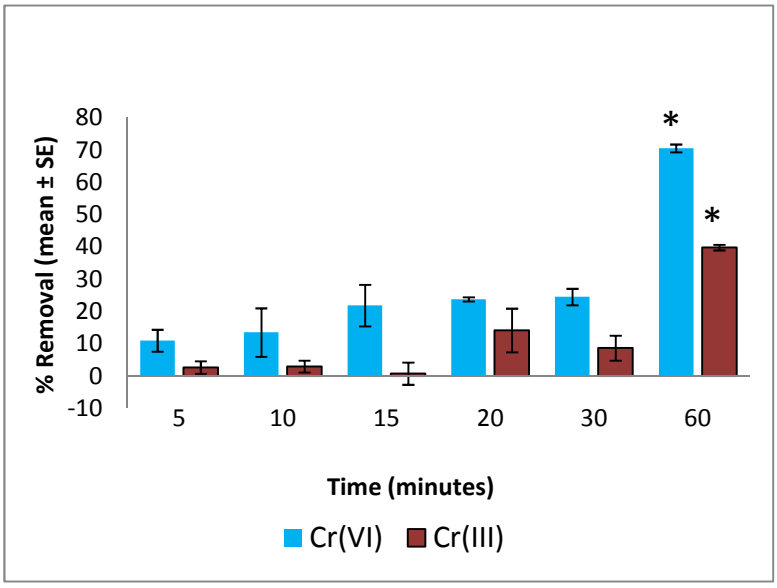

Fig 3.3 Time dependence of Cr(VI) and Cr(III) adsorption at a concentration of 100ppb and pH 4 to Jacobsite. Error bars represent ± standard error. * indicates statistical differences ($p<0.05$). Comparisons were made within the Cr(VI) study and a separate one within the Cr(III) study.

3.3.4 Adsorption isotherms

This study as explained in the previous chapter was to determine the amount of Cr(VI) and Cr(III) that could be adsorbed on to the nanomaterial. The isotherms were fitted using the Langmuir isotherm equation, as shown below in the linearized format:

$$\frac{C_e}{Q_e} = \frac{1}{(bQ_m)} + \frac{1}{(Q_m)} C_e$$

Where C_e is the equilibrium concentration of the Cr(VI) in solution, b is a constant that is related to the ionic strength and the pH of the solution. Q_m is the capacity of the material. The capacities determined using the Langmuir equation are Shown in Table 3.1.

Table 3.1. Cr(VI) and Cr(III) binding capacities to the Jacobsite nanophase based on different solution concentrations.

Sample	Capacity (mg/kg)	SE (+/- mg/kg)
$MnFe_2O_4$ Cr(VI)	1250	12.9
$MnFe_2O_4$ Cr(III)	370.3	23.7

The capacities for this experiment were 1250 mg/kg for hexavalent chromium and 370.3 mg/kg for trivalent chromium (1.25 mg/g and 0.37 mg/g, respectively). Hu et al. [6] reported that the capacity from their Jacobsite experiments was 31.55 mg of Cr(VI)/g of sorbent. Other materials, mainly synthetic, have also been experimented for sequestering chromium. In the study by Anabia et al. [7] they reported 128.2 mg/g, 153 mg/g for MCM-41, and MCM-48, respectively, at a pH range of 1-3. Another study showed an iron nanowire material that displayed a maximum capacity of 7.78 mg/g [14]. A similar material, γ-Fe_2O_3 in the nanophase, has been studied for the removal of Cr(VI) from aqueous solution at pH 2.5 [15]. The observed capacity of γ-Fe_2O_3 nanoparticles was 15.6 mg/g. On anatase, another oxide material, the capacity has been observed to be 14.56 mg/g [15]. The lower capacities in the current studies may be due to the pH of the solution and the amount of dissolved iron in the solution.

3.3.5 Interference studies

The interaction between the Jacobsite particles and the spiked chromium solutions are illustrated in Figures 3.4-3.7. The concentration ranges for the Cl^-, NO_3^-, SO_4^{2-}, and PO_4^{3-} range from 0.1 ppm to 100 ppm. As illustrated in Figures 3.4 and 3.5 for chlorine and nitrate respectively, the binding for Cl^- was approximately 100% at all the concentrations, with only a

small decrease of approximately 2% for the hexavalent chromium. The same was observed for the trivalent chromium, with the exception of the 2% decrease. Only a 1% decrease was observed at the 10 ppm and as the concentration of Cl increased the binding stayed constant. In terms of the nitrate anion, the binding showed a similar trend as it remained constant at 99% for the 0.1 and 10 ppm range. But then a small decrease occurred at the higher concentration of nitrate which resulted in a 95% removal of Cr(VI). The trivalent solution displayed constant binding in the presence of the nitrate anion solution. In terms of the sulfate anion and Cr(VI), the lower concentration of 0.1 showed only 90% binding. Subsequently, an increase in binding was observed when the concentration of interfering anions was increased. The remaining concentration range (1 ppm-100 ppm) showed a constant binding, which was 100%. A constant change in binding was observed between the different concentrations of the interfering anion and the trivalent chromium solution, starting at 100% then jumping down to 97%, back up to 100% and then to 97% for 0.1 ppm, 1 ppm, 10 ppm, and 100 ppm, respectively.

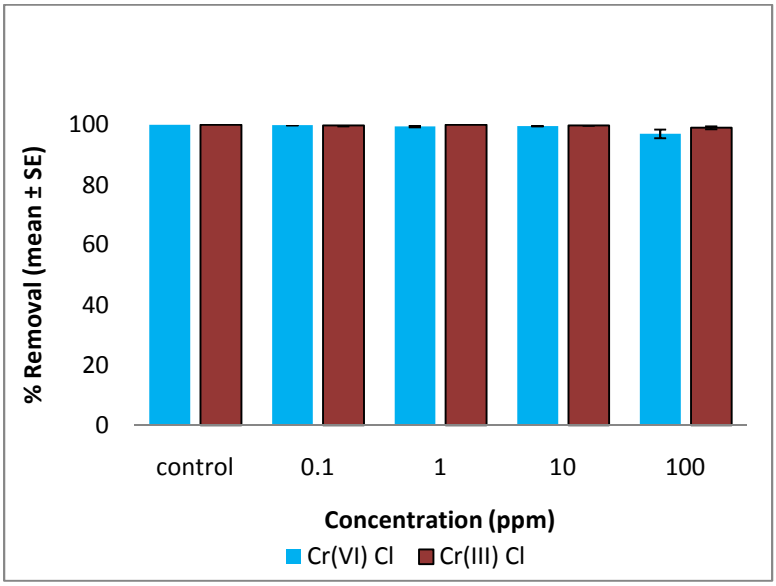

Fig 3.4. Sorption of Cr(VI) and Cr(III) at 100 ppb to the Jacobsite nanophase at different concentrations of chloride anion. Error bars represent ± standard error. Comparisons were made within the Cr(VI) study and a separate one within the Cr(III) study.

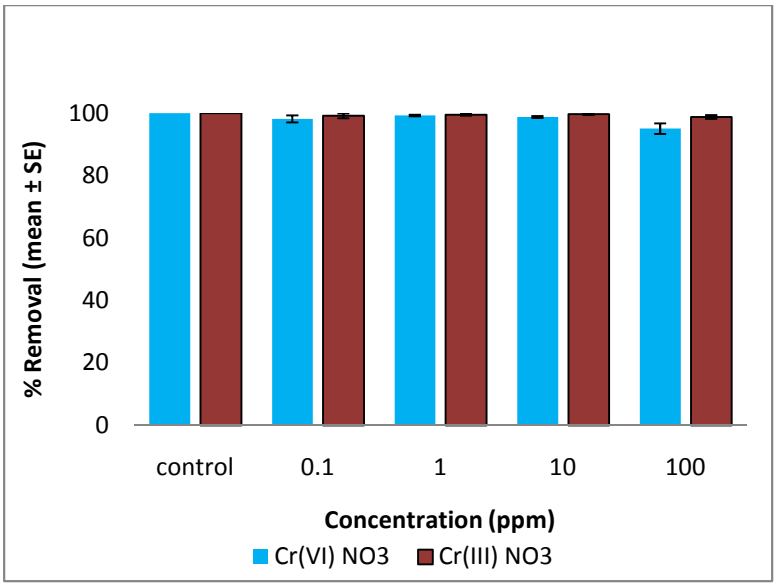

Fig 3.5. Sorption of Cr(VI) and Cr(III) at 100ppb to the Jacobsite nanophase at different concentrations of nitrate anion. Error bars represent ± standard error. Comparisons were made within the Cr(VI) study and a separate one within the Cr(III) study.

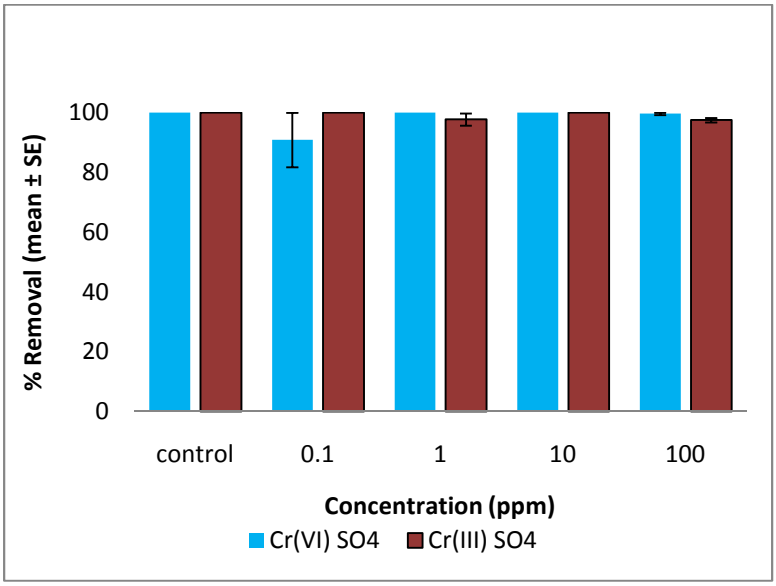

Fig 3.6. Sorption of Cr(VI) and Cr(III) at 100ppb to the Jacobsite nanophase at different concentrations of sulfate anion. Error bars represent ± standard error. Comparisons were made within the Cr(VI) study and a separate one within the Cr(III) study.

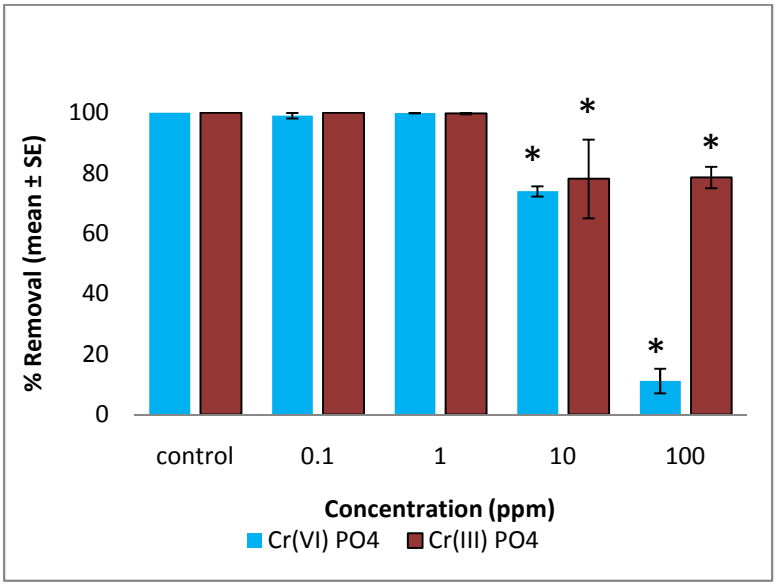

Fig 3.7. Sorption of Cr(VI) and Cr(III) at 100ppb to the Jacobsite nanophase at different concentrations of phosphate anion. * indicates statistical differences ($p<0.05$). Comparisons were made within the Cr(VI) study and a separate one within the Cr(III) study.

The phosphate showed interesting results in that both the trivalent and hexavalent solutions showed constant binding (100%) for the lower concentrations of interfering anion which could be due to a negative surface modification on the surface of the Jacobsite. When the concentration of interfering anion increased the binding decreased which could be due to complexing between the Cr(III) and the phosphate anions at the 10 ppm concentration, the binding was observed to be at 73% and 78% for Cr(VI) and Cr(III), respectively. Then at the 100 ppm concentration the binding stayed constant for the trivalent chromium (78%). However, for the hexavalent chromium, the concentration decreased significantly to 11% could possibly due to a negative surface forming on the surface of the Jacobsite, which is repelling the Cr(VI). The binding of both chromium species to Jacobsite was constant for all the different common anions, with the exception of phosphate which showed a significant difference at the 10 and 100

ppm concentration ranges for both Cr ions. As stated in the previous chapter chloride and fluoride anions do not inhibit the binding of Cr in different metal oxides which could be to the structure in solution or their low charge density. Sulfate and phosphate anions in Cr solutions have been known to reduce the binding of Cr(VI) between different oxide materials and Cr(VI) [15-16]. With the exception of the 100 ppm phosphate-hexavalent chromium experiment, the Jacobsite shows preferential binding to both chromium species in the presence of different competing anions.

3.4. Conclusion

Jacobsite proved to be an acceptable agent for the sequestering of Cr(VI) and (III). Different tests were performed in order to determine that the material was indeed Jacobsite and the size of the material was 12 nm. The data obtained from the interference studies showed that in the presence of competing ions the material displayed 100% binding for Cl^-, NO_3^- and SO_4^{2-}. In the presence of high concentrations of PO_4^{3-} the binding reduced to possible complexing between the Cr(III) and the phosphate anion. In the case of Cr(VI) the Jacobsite could be forming a negative layer from the precipitation of the phosphate onto the surface of the material resulting a repulsion between the charge of the phosphate anion and the negatively charged surface of the Jacobsite.

4. Sorption of Cr(III) and Cr(VI) to High and Low Pressure Synthetic Nano-Hausmannite (Mn_3O_4)Particles

Abstract

Hexavalent and trivalent chromium are the two most stable ions that result from the use of Chromium. Cr(III) is an essential trace element for mammals. Cr(VI) on the other hand is extremely carcinogenic to most organisms. In this study an investigation was conducted on the binding of Cr(III) and Cr(VI) to an engineered nanomaterial, Hausmannite, which we have synthesized using two different synthesis techniques. One of the techniques utilized a simple titration/precipitation synthesis involving the titration of manganese(II) sulfate with sodium hydroxide at a molar ratio of 3 (OH): 1 Mn ion. The samples were aged using different techniques. The open vessel ageing technique used was a heating mantle and the nanomaterial was heated 90ºC for 60 minutes. The microwaved ageing technique was performed using closed vessels containing the materials which were heated to 90ºC for 30 minutes. The batch studies showed the micro-waved material had a binding of 85% and 87% for Cr(VI) and Cr(III) at pH 4 and the open system Hausmannite showed a 75% and 77% removal for Cr(VI) and Cr(III) respectively. The optimum time for both Hausmannite materials to effectively bind to Cr(VI) and Cr(III) was 1h. The closed system and open system Hausmannite showed binding capacities (mg/kg) of 400 and 500 for Cr(VI) and 2857.1 and 4761.9 for Cr(III), respectively. Finally data was obtained from the interaction of the Hausmannite and chromium when competing anions were introduced.

4.1. Introduction

Many methods exist to remove the two chromium species, some are natural and synthetic iron oxide nanomaterials, other methods are synthetic organic compounds [1-5]. One possible method for sequestering hexavalent chromium could be manganese oxide nanophases in the form of Mn_3O_4. Currently one method using mesoporous materials showed effective binding capacity of 128.2 and 153.8 mg/g respectively [6]. Another method of removing Cr(VI),was the use of a manganese nodule leached residue obtained from NH_3–SO_2 leaching showed a binding capacity of 22.47 mmol/g [7]. Perhaps the largest advantage of using the manganese oxide materials is that the possible dissolution would release manganese into solution, which is an essential nutrient. It has been known that iron based materials tend to reduce hexavalent chromium to trivalent oxidation state [8-9].

The current study showed the binding trends of the Hausmannite nanomaterials and the chromium solutions at pH values ranging from 2-6. The next step in the study was to determine the amount of time required for the chromium to bind to the Hausmannite under the optimum pH conditions. Furthermore the binding capacity of the nano-Hausmannite was determined using the Langmuir isotherm model. The nanomaterials were then tested using chloride, nitrate, sulfate, and phosphate anion spiked chromium solutions to test the materials effectiveness in the presence of competing ions , then all the supernatants were analyzed using a graphite furnace to identify how much of the chromium ions remained in solution.

4.2. Methodology

4.2.1. Synthesis of manganese oxide nanoparticles

The synthesis of this material was achieved using the same method as described in chapter 2, with the only exception being the salts used for the making the nano-Hausmannite. The amount of salt used was 5.07 g of manganese sulfate monohydrate and it was dissolved in 1.0 L of DI water. The solution was then titrated with a 1M solution of sodium hydroxide. The aging technique used for the formation of the nano-Hausmannite was the exact method described in chapter two for the aging of the nano-Magnetite.

The batch studies (pH, time dependency, binding capacity and interference studies) performed on the nanomaterials were described in previous chapters. The same characterization studies were also performed on the Hausmannite material in order to determine the crystal structure and other characterization properties.

4.3 Results and Discussion

4.3.1. XRD data

The manganese oxide particles underwent XRD studies and the results from this study determined that the particles were indeed Hausmannite (Mn_4O_3) and after utilizing Scherrer's equation, the average particle size of the nano-Hausmannite was approximately 34 nm for the micro waved closed vessel particles and 25 nm for the open vessel synthesized particles which were on par with Parsons et al. [12].

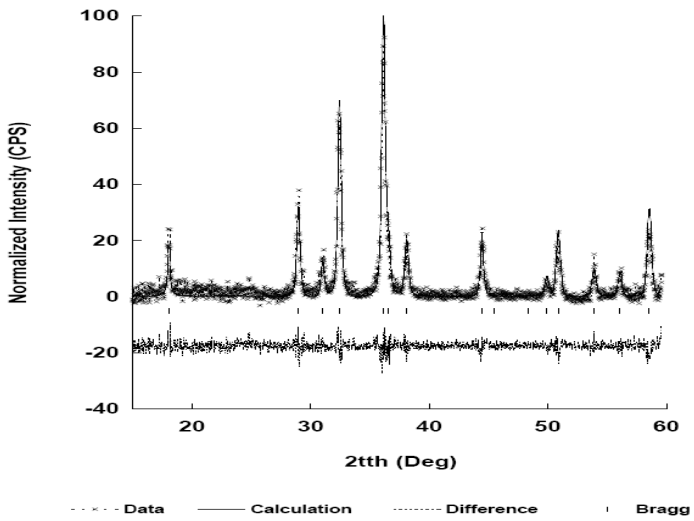

Fig 4.1. Diffraction pattern of nano-Hausmannite from 20° to 60°.

4.3.2. pH study

The pH profiles are illustrated in figures 4.2 and 4.3; they display both sets of particles with the two different chromium ions. For the microwave material, the removal of hexavalent chromium was 85% at pH 3 and remained relatively constant at pH 4 and 6, with a minimal decrease at pH 5. Similarly, the micro-waved aged material displayed an 87% removal of the trivalent chromium from solution at pH 3 and remained constant their after. On the other hand, the open vessel material exhibited a binding of 75% with the Cr(VI) at lower pH and remained constant at higher pH levels, but at pH 5 and 6, the binding decreased to about 65%. The binding for Cr(III) at lower pH levels was about 78% binding and remained constant until higher pH levels displayed a decrease in binding. Other studies have also reported similar trends in the binding of Cr(VI) to other oxide materials [13].

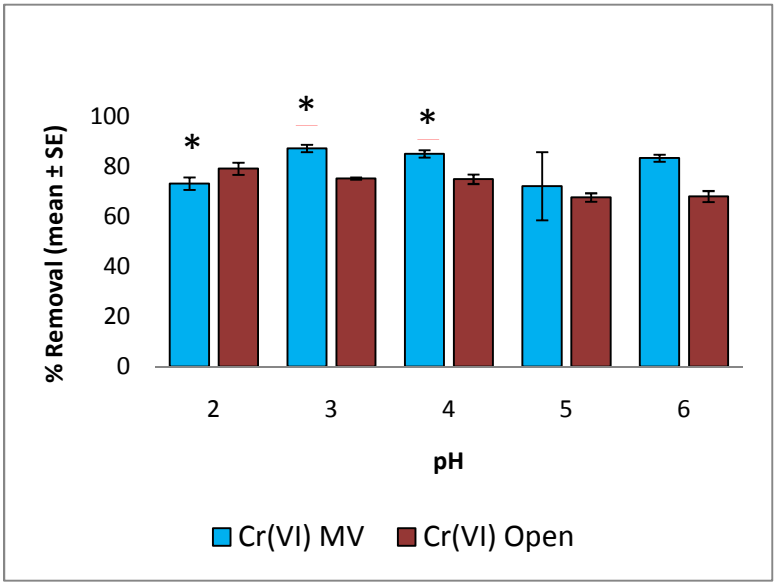

Figure 4.2 Sorption of Cr(VI) to open and closed system Hausmannite at pH 2-6. Error bars represent ± standard error. * indicates statistical differences ($p<0.05$). Comparisons were made within the microwave material (MV) and open (non-microwave) material.

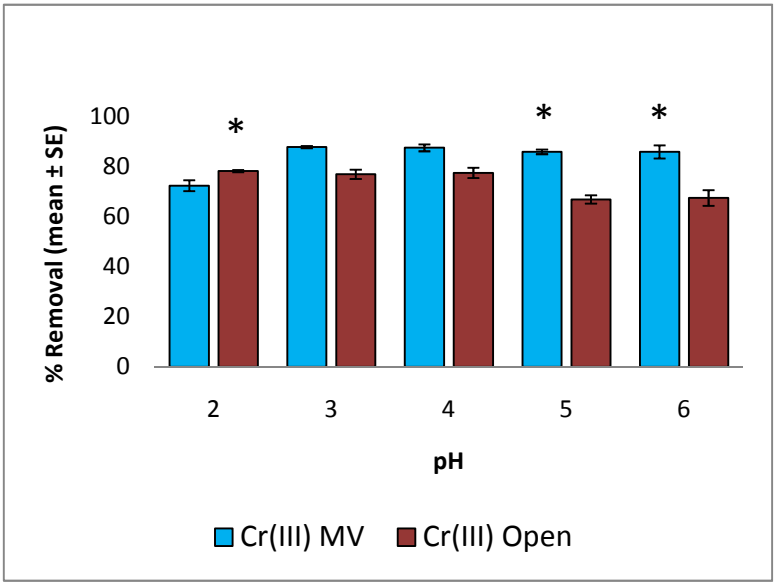

Figure 4.3. Sorption of Cr(III) to open and closed system Hausmannite at pH 2-6. Error bars represent ± standard error. * indicates statistical differences ($p<0.05$). Comparisons were made within the microwave material (MV) and open (non-microwave) material.

4.3.3. Time dependency study

Figure 4.4 and 4.5 shows the time dependency of the binding of both chromium ions to the open vessel and microwave assisted synthesized Mn_3O_4 nanomaterials. The Cr(VI) bound rapidly to the microwave assisted synthesized Mn_3O_4, (within the first 5 min) and remained constant for up 1 h after contact. The interaction between the microwave aged nanoparticles and Cr(VI) exhibited a stable binding at the first 5 min, but the binding was relatively low 24%, then as time increases the binding begins to decrease to approximately 19%. When the reaction time increased further, the binding increases to 33% and remains constant till the 1 h mark. At 1 h binding increases dramatically to 85%.

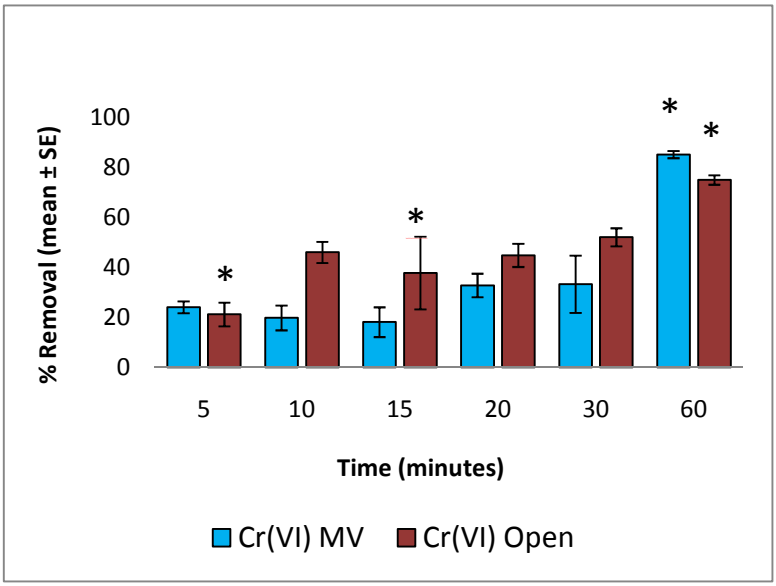

Figure 4.4. Time dependence of Cr(VI) adsorption at a concentration of 100ppb and pH 4 to open and closed system Hausmannite. * indicates statistical differences ($p<0.05$). Comparisons were made within the microwave material (MV) and open (non-microwave) material.

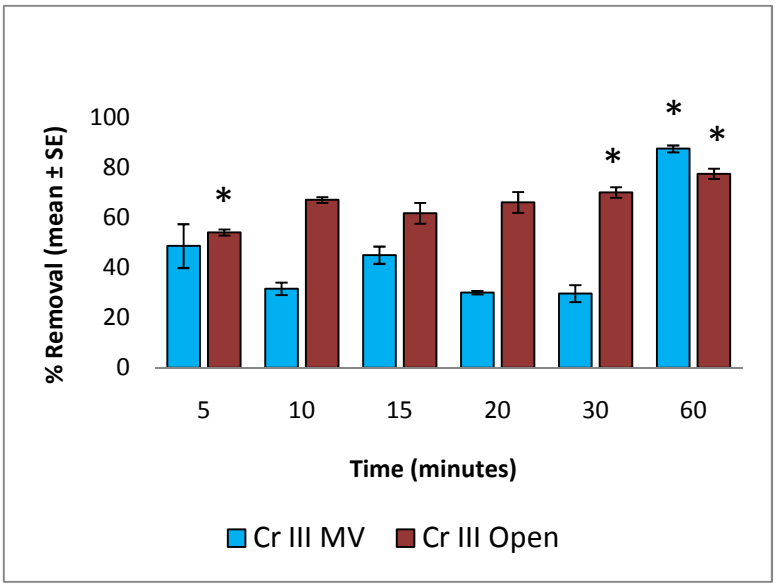

Figure 4.5 Time dependence of Cr(III) adsorption at a concentration of 100ppb and pH 4 to open and closed system Hausmannite. Error bars represent ± standard error. * indicates statistical differences ($p<0.05$). Comparisons were made within the microwave material (MV) and open (non-microwave) material.

The binding for the open vessel material peaked at 1h and the binding that resulted from the reaction was approximately at 75%, which deviates from the trend that was shown for the microwave material at the 1 h mark possibly could be due to different redox reactions occurring between the material and the metal ion, thus in order to overcome this, equilibrium needs to be established between the material and the ion. For the Cr(III) experiments, the binding trends that were observed for the microwave nanomaterial were of an alternating nature. At the first five minutes the binding displayed approximately 48% removal and then at the ten minute mark the binding decreased to 31% then this alternating trend was constant afterwards until the one hour mark. For the open vessel material the binding trend displayed 50% binding in the first five minutes, then it constantly increased as the time increased. The binding peaked at 78% and remained constant after 1h. However, Cr(VI) generally requires more time to bind than Cr(III)

due to different redox reactions involving the manganese and the oxygen found on the surface of the material [14].

4.3.4. Adsorption isotherm

As described in the previous chapter the isotherms were fitted using the Langmuir isotherm equation as shown below in the linearized format:

$$\frac{C_e}{Q_e} = \frac{1}{(bQ_m)} + \frac{1}{(Q_m)} C_e$$

Where C_e is the equilibrium concentration of the Cr(VI/III) in solution, b is a constant that is related to the ionic strength and the pH of the solution and Q_m is the capacity of the material. The capacities determined using the Langmuir equation are shown in Table 4.1.

Table 4.1. Cr(VI) and Cr(III) binding capacities based on different solution concentrations to both open and closed system Hausmannite

Sample	Capacity (mg/kg)	SE (+/- mg/kg)
Mn_3O_4 Cr(VI) MV	400	72.5
Mn_3O_4 Cr(VI) Op	500	5.9
Mn_3O_4 Cr(III) MV	2857.1	55.1
Mn_3O_4 Cr(III) Op	4761.9	152.9

The capacities for the microwave nanomaterial were 0.400 mg/g and 2.857 mg/g for Cr(VI) and Cr(III) respectively. The capacities for the open vessel material were 0.500 mg/g and 4.761

mg/g for Cr(VI) and Cr(III) respectively, the low capacity of Cr(VI) suggests that Hausmannite may have possibly undergone reductive and oxidative dissolution of the mineral phases thus resulting in low capacity [11]. Komosinska reported that alder peat and brown coal displayed binding of 20.200 mg/g and 39.370 mg/g respectively [15]. Correra reported that the binding of boehmite and hexavalent chromium was to at 0.001598 mg/g [16]. Anabia et al. reported 128.2 mg/g and 153 mg/g for MCM-41 and MCM-48 respectively at a pH range of 1-3 [6]. In some similar iron nanomaterials the capacities exhibited were 15.6 mg/g for γ-Fe_2O_3 and on anatase another iron based material the capacity has been observed to be 14.56 mg/g [17].

4.3.5. Interference study

Figures 4.6-4.9 show the effects of (Cl^-, NO_3^-, SO_4^{2-} and PO_4^{3-}) competing ions have on the binding of Cr(VI) and Cr(III) to the open and closed system Hausmannite at pH 4. The concentrations of the common ions in the solutions were on the range of 0.1 ppm to 100 ppm. The first set of interactions was that of the chlorine spiked hexavalent solutions with the microwave aged nanomaterials which displayed a constant binding trend at around 67% with respect to the increasing concentration of the interfering anion. In the case of the open vessel material the binding was lower than the binding observed for the microwave aged materials. The binding peaked at 40% for Cr(VI) at low concentrations of chlorine anion as seen in Figure 4.6 A. The trends observed in the experiments between the micro-waved synthesized nanomaterials and the chlorine spiked trivalent solutions showed low binding for all concentrations of interfering anion which could be caused by complex formation between the Cr(III) and the saturation of chlorine ions on the surface of the nano-Hausmannite therefore inhibiting the binding to Cr(III). The interaction between the open particles and the spiked solutions showed 100% binding at all concentrations of the competing anions as seen in Figure 4.6 B. The next

interfering anion to be tested was the nitrate anion which has the same charge as chlorine but is larger in size.

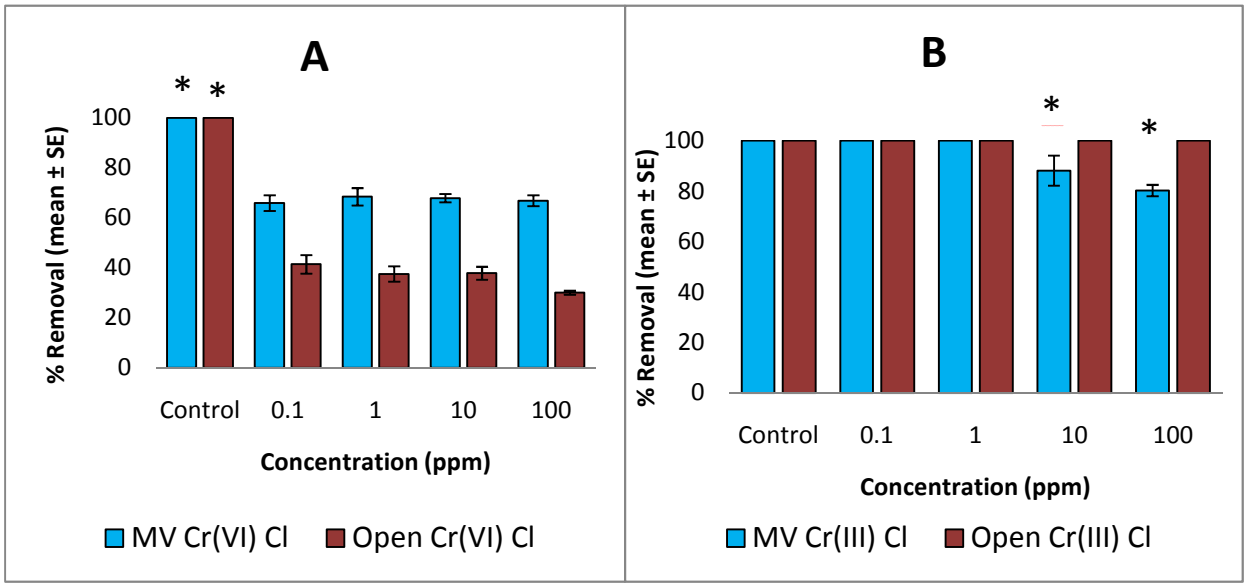

Fig 4.6. Sorption of (A.) Cr(VI) and (B.) Cr(III) at 100 ppb to the Hausmannite nanomaterial at different concentrations of chloride anion. Error bars represent ± standard error. * indicates statistical differences ($p<0.05$). Comparisons were made within the microwave material (MV) and open (non-microwave) material.

For the nitrate study, both sets of particles interacted with the nitrate spiked Cr(VI) solutions showed a constant binding of approximately 70% and 35% for the micro-waved hausmannite and the open vessel hausmannite respectively as seen in Figure 4.7 A. Both sets of materials showed a small decrease in binding as the concentrations of anion increased, but ultimately the binding began to increase as the concentration increased to higher levels of anion. The hexavalent chromium displayed an affinity to bind to the micro-waved material of the open vessel material which could be a result of the aging method forming an acidic layer on the surface of the material.

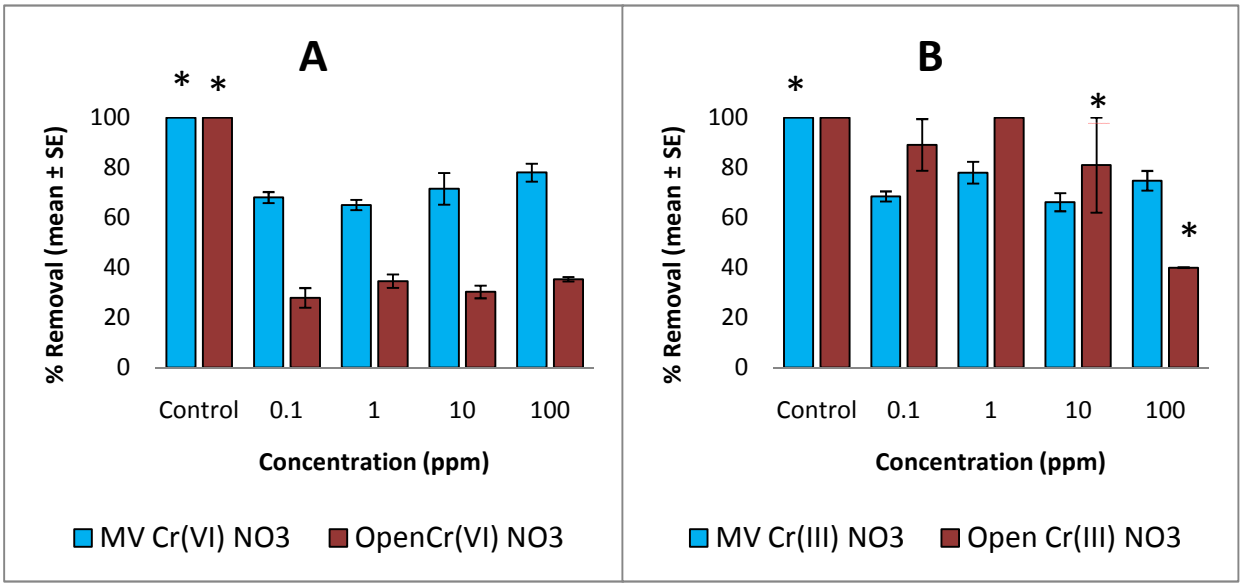

Fig 4.7. Sorption of (A.) Cr(VI) and (B.) Cr(III) at 100ppb to the Hausmannite nanophase at different concentrations of nitrate anion. Error bars represent ± standard error. * indicates statistical differences ($p<0.05$). Comparisons were made within the microwave material (MV) and open (non-microwave) material.

The nitrate spiked Cr(III) solutions showed a similar trend to the hexavalent studies, but the trivalent chromium preferred to the open vessel materials over the micro-waved materials as seen in Figure 4.7 B. For the micro-waved particles, as the concentration of interfering anion increased the binding would increase and decrease by 10%. The open vessel particles showed a constant binding trend above 80%, but at high levels of competing anion, it decreased to 40%, this binding trend suggests that nitrate in large concentrations overpower the Cr(III) due to nitrates structure, thus making the search for chromium difficult for the nanomaterial.

The next anion was sulfate, which like nitrate is a polyatomic anion, but it has a -2 charge. Both sets of particles showed a decreasing binding trend as the anion concentration increased. Cr(VI) showed a preference (similar to the nitrate experiment) to the micro-waved

system then the open vessel system as seen in Figure 4.8 A. The trivalent chromium solution showed a similar trend as seen in the Cr(VI) study, but the binding was constant for the majority of the different concentrations. Both sets of particles showed a decrease in binding at the 100 ppm level of competing anion. The only difference was that the open particle binding was 10% lower than the micro-wave results. The next competing anion was phosphate, which has a more negative charge then the chromate anion and even more negative then the chromium 3+ species in the trivalent solution. The polyatomic anion also possess a tetrahedral shape, but to further exacerbate the trend the phosphate anion promote a -3 charge which further decreases binding. Overall for both sets of tests, as can be seen in Figures 4.9 A and B the overall trend for binding was a decreasing one, as the interfering anion increased in concentration the bind decreased significantly. The highest % of binding occurred at the lower concentrations of competing anion, for both Cr(VI) and Cr(III). For Cr(VI), the micro-waved particles demonstrated more binding to the chromium possibly due to as the nature of the nano-Hausmannite surface explained in the chloride experiment. At higher levels of concentrations the phosphate could have precipated onto the surface of the material and repel the anionic chromate. There have been studies that show that fluorine and chlorine show little to no interference when it interacts with both species of chromium and iron oxide materials [18]. The sulfate and phosphate anions have both been determined to hinder the binding between oxide materials and chromium ions. This could be due to the robust structure and larger anionic charge of the anion. Another factor could be the possibility of surface modification on the material [18-19].

4.0 Conclusion

The micro-waved Hausmannite seemed to bind better to the Cr(III), than the Cr(VI) as seen in the binding capacity data. The nano-Hausmannite showed a capacity of 2857.1 mg of

Cr(III)/kg of material and 4761.9 mg of Cr(III)/kg of material compared to 500 and 400 mg of Cr(VI)/kg of material. Thus Hausmannite could be a possible sequestering agent for the filtration of trivalent chromium. On the other hand, the open vessel particle showed slightly less binding possibly due to the nature of its surface. Overall the Hausmannite mineral showed that it indeed have an affinity to the chromium. The materials themselves are relatively inexpensive. The material showed its ability to maneuver through some of the competing anions, but as the concentration of anion increased the binding decreased. This could be due to synergistic effects or the larger charges that are found in some of the competing anions. At different concentrations of interfering anion the nano-Hausmannite displayed more that 50% binding.

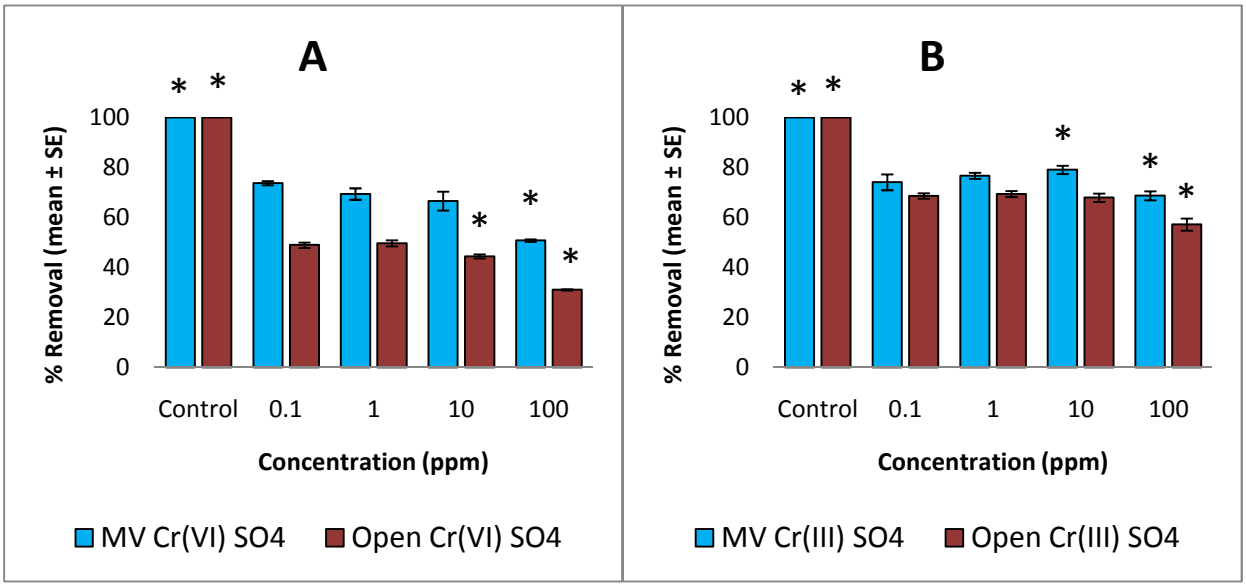

Fig 4.8. Sorption of: A. Cr(VI) and B. Cr(III) at 100ppb to the Hausmannite nanophase at different concentrations of sulfate anion. Error bars represent ± standard error. * indicates statistical differences ($p<0.05$). Comparisons were made within the microwave material (MV) and open (non-microwave) material.

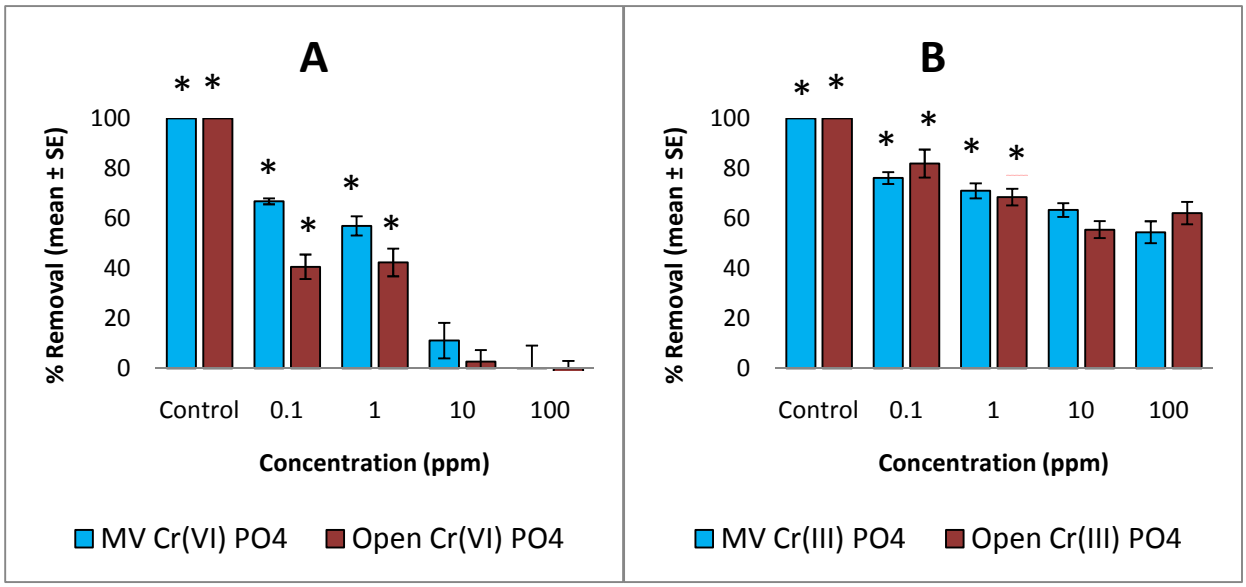

Fig 4.9 Sorption of (A.) Cr(VI) and (B.) Cr(III) at 100ppb to the Hausmannite nanophase at different concentrations of phosphate anion. Error bars represent ± standard error. * indicates statistical differences ($p<0.05$). Comparisons were made within the microwave material (MV) and open (non-microwave) material.

5. X-ray Absorption Spectroscopy Studies of the Adsorption of Iron and Manganese Oxide Nanomaterials to Cr(VI) and Cr(III)

Abstract

Chromium has two abundant oxidation states that are found in the environment: Cr(VI) and Cr(III). Cr(VI) is very carcinogenic to mammals while Cr(III) is an essential trace element for sugar and lipid metabolism. In order to fully understand how both chromium ions would be affected by coming in contact with iron and manganese oxide nanomaterials, the binding mechanism must be studied. An effective method for studying the adsorption mechanism is the X-ray absorption near-edge structure (XANES) spectroscopy. XANES spectra were obtained from non microwave-assisted and microwave-assisted, synthetic Fe_3O_4, Mn_3O_4, and $MnFe_2O_4$ nanomaterials that were reacted with solutions of both chromium ions. The chromium solutions were pH-adjusted to 2, 4, and 6. It was determined that the Cr(VI) solutions that came into contact with the Fe_3O_4 and Mn_3O_4 reduced to Cr(III); however, the Cr(VI) solutions that reacted with $MnFe_2O_4$ remained as Cr(VI). The Cr(III) remained as Cr(III).

5.1 Introduction

Some XAS studies have been conducted on this material and several of its engineered variants, all of which concluded that upon contact with Magnetite, Cr(VI) reduces to Cr(III) through the exchange of electrons from the Fe(II) found in the crystal structure of the Magnetite [1-2]. Another possible candidate material for the sequestering of both chromium species is Jacobsite ($MnFe_2O_4$), which currently has a limited number of publications. Hu et al. reported that while Jacobsite was a good material for sequestering Cr(VI), it did not reduce the Cr(VI) to Cr(III) [3]. The authors theorize that the bond between the oxygen from the chromate and the Fe/Mn layer was relatively weak in comparison to the bond found between the oxygen in the chromate and the Fe(II) found in Magnetite. Currently, there are no publications of any kind on the subject of the interaction between both chromium species and the nanomaterial Hausmannite.

In the present study Cr(VI) and Cr(III) adsorption to non microwave-aged and microwave-aged Fe_3O_4 and Mn_3O_4, and microwave-aged synthetic $MnFe_2O_4$ nanomaterials was investigated using synchrotron-based XAS. The oxidation state of the chromium ions adsorbed to the surface of the oxide nanomaterials was determined by XANES spectroscopy after the two chromium species reacted with the different materials at a set pH range (e.g. 2, 4, and 6).

5.2 Methodology

5.2.1. Sample preparation

In this study 100 ppb solutions of both Cr(VI) and Cr(III) were made using reagent grade potassium dichromate ($K_2Cr_2O_7$) and chromium nitrate ($Cr(NO_3)_3$), respectively. These

solutions were then pH-adjusted to 2, 4, and 6 using dilute sodium hydroxide and hydrochloric acid. The synthesis of the non microwave-aged and microwave-aged Fe_3O_4 and Mn_3O_4, and microwave-aged synthetic $MnFe_2O_4$ nanomaterials were prepared using the same method as described in chapters 2-4. 10 mg of either Fe_3O_4, Mn_3O_4, or $MnFe_2O_4$ were weighed and put into 5mL polyethylene test tubes. Then they were introduced to 4mL of either chromium solution at pH 2. The same was done for the other pH-adjusted solutions. The samples were rocked (Specimix, Thermo Scientific) for 1h and centrifuged for 10 min at 3000 rpm. Once centrifuged, the supernatants were discarded and the solids were oven dried for analysis. This analysis was conducted at Stanford Synchrotron Radiation Lightsource (SSRL, Palo Alto, CA).

5.2.2. XANES study

The XANES studies to investigate the oxidation state of chromium adsorbed at the nanomaterials surface and possible bonding mechanisms were performed at SSRL on Beam Line 7-3 using a liquid helium cryostat (4-200 K). The operating conditions of the beam line were 3 GeV energy with a beam current of 50-100 mA. A Canberra 29-element array germanium detector and Si(220) φ 90 monochromator were used to obtain the fluorescence spectra for the Cr-K edge spectra. The model compounds used for comparison of the spectra were potassium dichromate and chromium nitrate. A chromium foil [Cr(0)] was used as a calibration standard to determine the correct edge energy of samples. Spectra of oxide material samples and chromium model compounds were collected using the Cr-Kα 5989eV.

5.3. Results and Discussion

5.3.1 Results of XANES studies

Figures 5.1-5.3 show the XANES spectra for the different materials that were reacted with both chromium species. The prevalent characteristic in a Cr(VI) XANES spectra is the sharp peak that is located at 5989eV, known as the pre edge, due to the forbidden electron transition that occurs when the X-ray photon excites a k-shell electron (requiring a large amount of energy). In Figure 5.1A and C displays the oxidation state of the Cr that was reacted with both the micro-waved and open synthesis Magnetite nanomaterial the pre edge of all the spectra did not show the characteristic Cr(VI) pre edge that is prevalent in the Cr(VI) XANES spectra. The spectra displayed a very small peak at the chromium pre edge, which is characteristic of the Cr(III) ion. The peak did on the other hand display a sharp characteristic much like the Cr(VI) which could mean there is a relatively small amount of un-reacted Cr(VI). Much like the experiment performed by White and Peterson, the Magnetite, both microwave-aged and non microwave-aged, reduced the Cr(VI) to Cr(III) [1-2]. In both of the Cr(III) reactions, the pH 2 solutions were too dilute and could not be analyzed in the synchrotron.

Figure 5.2 displays the XANES spectra for the microwaved and the non microwaved Hausmannite nanomaterial. Like the Magnetite nanomaterial, the peak found at 5989eV for all four spectra displayed characteristics of Cr(III) and not Cr(VI). Therefore, the Hausmannite behaves like the Magnetite. The logical explanation for reduction could have to do with the Mn(II) found in the Hausmannite crystal, which is undergoing a redox reaction and transferring electrons from the Mn(II) to the Cr(VI), thus behaving like the Fe(II) found in the Magnetite [1-2].

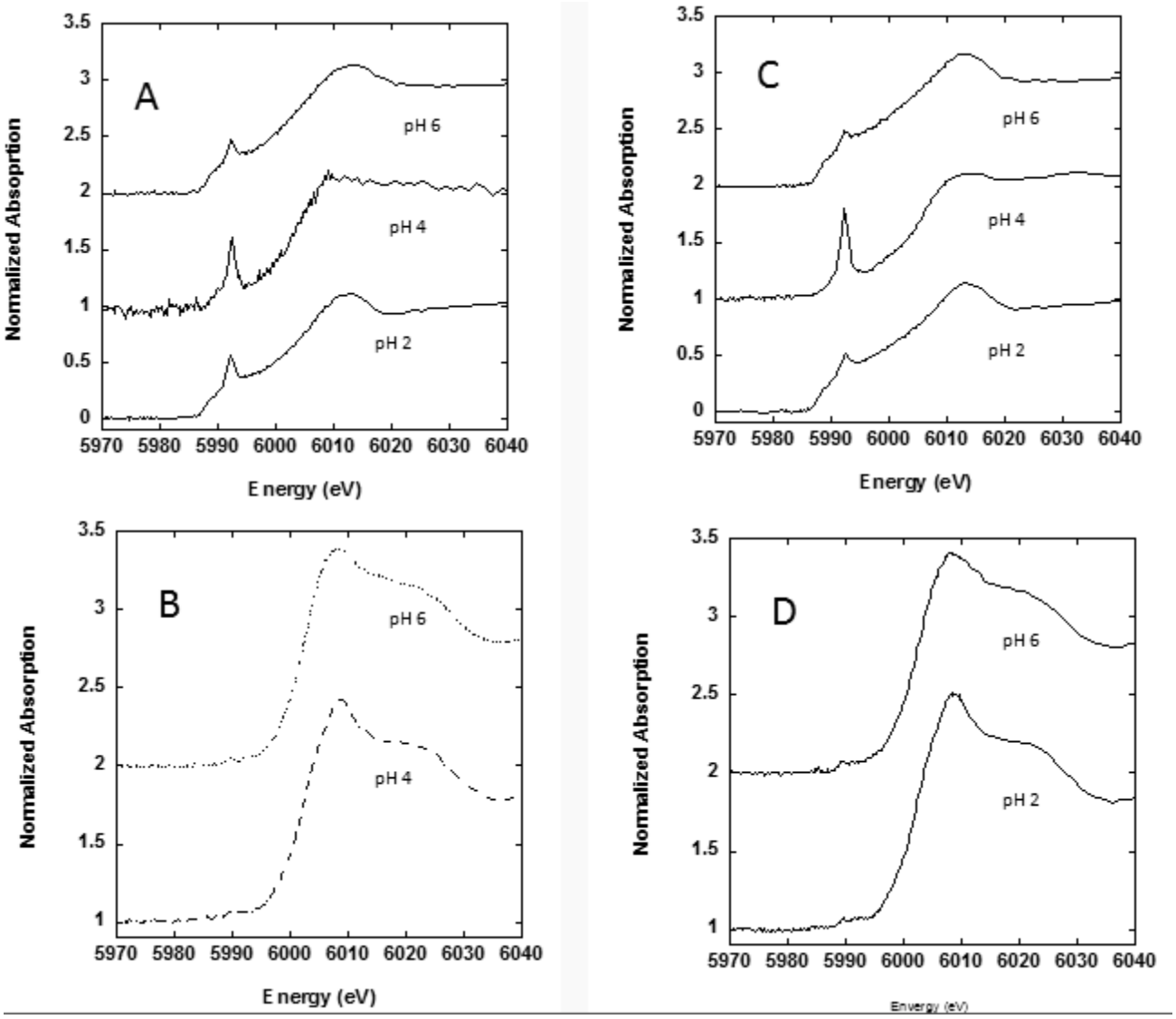

Figure 5.1XANES spectra of Cr(VI) and Cr(III) to microwave-aged and non microwave-aged Fe_3O_4. A) Cr(VI) with MW Magnetite, B) Cr(III) with MW Magnetite, C) Cr(VI) with NMW Magnetite, D) Cr(III) with NMW Magnetite.

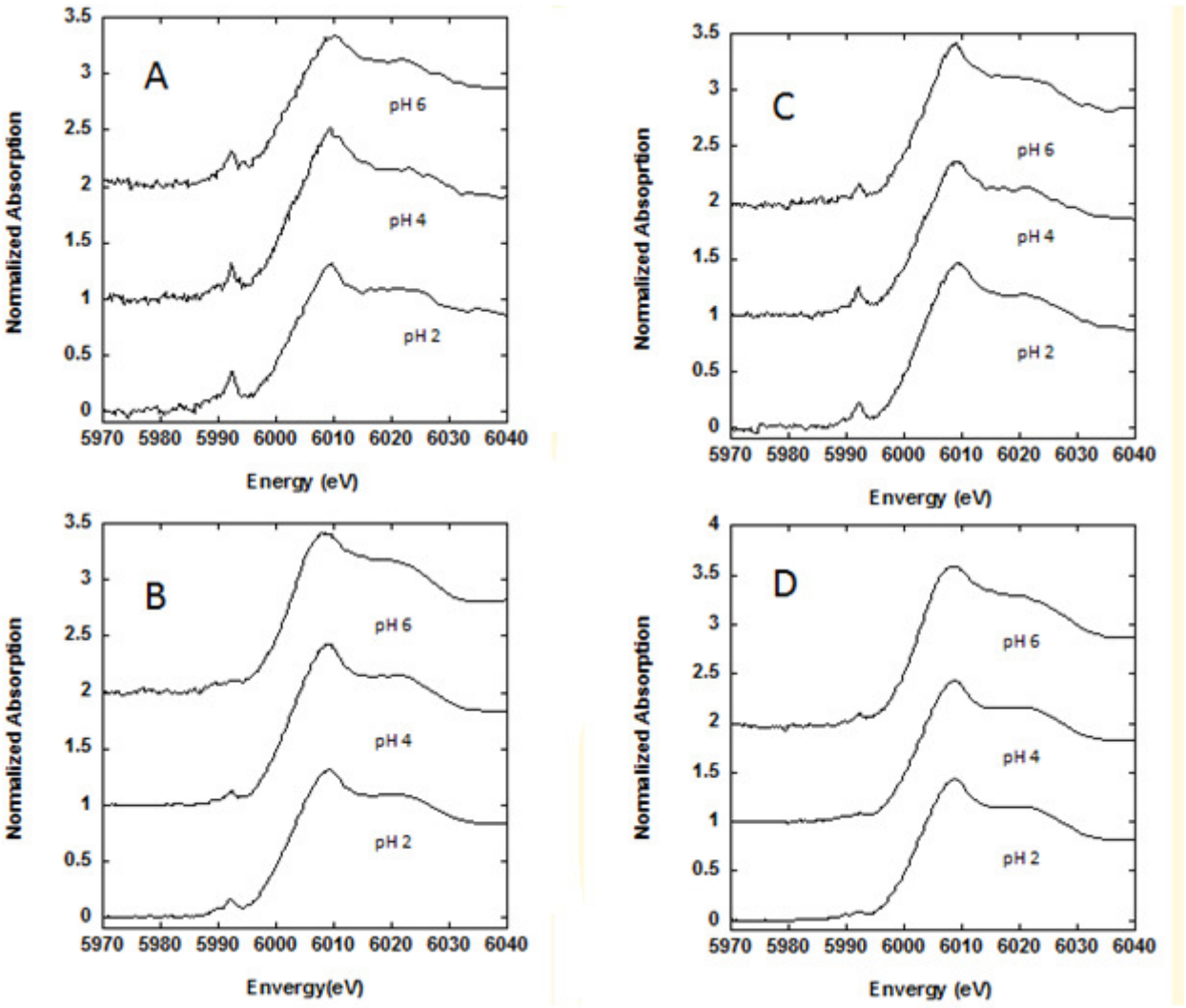

Figure 5.2. XANES spectra of Cr(VI) and Cr(III) to microwave-aged and non microwave-aged Mn_3O_4. A) Cr(VI) with MW Hausmannite, B) Cr(III) with MW Hausmannite, C) Cr(VI) with NMW Hausmannite, D) Cr(III) with NMW Hausmannite.

Figure 5.3 showed the XANES spectra for nano-Jacobsite. The spectra showed an interesting phenomenon that deviated from the other two experiments. The Cr(VI) reacted with the nano-Jacobsite remained as Cr(VI); there was no reduction present such as seen in the pre edge of the spectra. This result coincides with the study that was conducted by Hu et al. The authors explained that the reason for no reduction could be a result of the relatively weak bond

between the chromate and the surface of the material [3]. The weak bond cannot transfer the electrons from the Fe/Mn surface to the chromate [3]. The Cr(III) found on the Jacobsite remained as Cr(III).

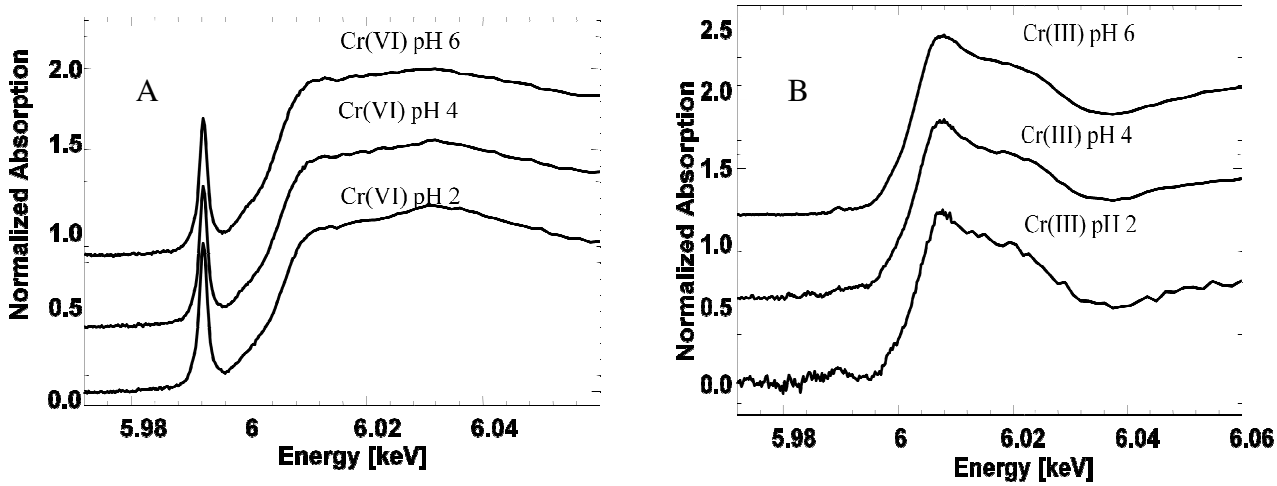

Figure 5.3 XANES spectra of (A.) Cr(VI) and (B.) Cr(III) bound to microwave-aged $MnFe_2O_4$.

5.4 Conclusion

The purpose of using XAS is to determine what type of binding is occurring within the samples upon contact time. The purpose of the XANES experiment is to determine the oxidation state after the sample is reacted. It was determined that two of the materials effectively reduced the Cr(VI) to Cr(III) in aqueous solutions. This phenomenon shows that using oxide nano-Magnetite and nano-Hausmannite can be an effective method for remediation of Cr(VI) in water. The nano-Jacobsite did not show any sort of reduction of Cr(VI) to Cr(III). This could be due to the type of bond exhibited by the chromate on the surface of the material. Nano-Jacobsite is still a very good material to use for the sequestering chromium from aqueous solutions.

6. Conclusions

Micro-wave and non micro-waved nanomaterials were tested for their capacity to remove Cr(III) and Cr(VI) from aqueous solutions . The XRD data showed that the overall crystal structures for all three different nanomaterials were in fact identical structures of Magnetite, Jacobsite and Hausmannite. The XRD also determined that the overall crystalline size of the three micro-waved aged materials and the two traditionally aged (open) materials were as follows: 25 nm for MW Magnetite, 34 for MW Hausmannite, 28 nm for open Magnetite, 25 nm for open Hausmannite, and finally 18 nm for the Jacobsite.

The data obtained from the XAS studies showed that Magnetite and Hausmannite both reduced the hexavalent chromium species into the trivalent species. The studies showed that the reduction process is a direct result of the binding of the Fe(II) species found within the Magnetite material and the Mn(II) species found within the Hausmannite nanomaterial. The XAS data showed that the Jacobsite nanomaterial, which has characteristics of both the Magnetite and the Hausmannite, showed no reduction of the hexavalent chromium to trivalent chromium.

At pH levels below 4 materials such as Magnetite and Jacobsite would dissolve as a result of high acidity. At higher pH levels it was determined that the materials exhibit an overall negative surface charge. This surface charge repels the negatively charged oxoanion, at lower pH levels that nanomaterials exhibit a neutral charged surface due to the abundance of hydrogen ions. This surface thus becomes littered with possible binding sites. It was determined that all three materials (Magnetite, Jacobsite, Hausmannite) successfully sequestered both chromium ions at a pH of 4. The overall contact time necessary for binding of the two chromium ions to the different nanomaterials was determined to be 1h and the overall capacities of the three three micro-waved aged materials and the two traditionally aged materials were as follows:

Sample	Capacity (mg/kg)	SE (+/- mg/kg)
Fe_3O_4 Cr(VI) MV	1208	43.9
Fe_3O_4 Cr(VI) Op	1705	14.5
Fe_3O_4 Cr(III) MV	555	10.5
Fe_3O_4 Cr(III) Op	555	2.2
$MnFe_2O_4$ Cr(VI)	1250	12.9
$MnFe_2O_4$ Cr(III)	370.3	23.7
Mn_3O_4 Cr(VI) MV	400	72.5
Mn_3O_4 Cr(VI) Op	500	5.9
Mn_3O_4 Cr(III) MV	2857.1	55.1
Mn_3O_4 Cr(III) Op	4761.9	152.9

The non micro-waved (open) aged Magnetite showed preferential binding to both the Cr(VI) and Cr(III) solutions compared to the micro-waved aged Magnetite which could be a result form the formation of an Fe(III) layer at the surface of the material during the aging process. In the interference study the competing ions displayed minimal effectiveness to the open vessel Magnetite in the Cr(VI) portion of the study, the particles showed 100% removal even in the presence of high concentrations of sulfate ion. The Cr(III) portion of the interference studies showed the Magnetite had no interference from the chlorine and high concentrations of sulfate ion thus resulting in high removal percentage possible through the formation of a charged surface from the excess of anions.

Jacobsite in the interference study showed that the competing ions showed no interference in the sequestering of both chromium ions except for high concentrations of phosphate anion. The micro-waved Hausmannite showed a preference to Cr(III) and Cr(VI) over the open synthesized Hausmannite. In all cases the reaction of the nano-Hausmannite with Cr(VI) in the presence of interference ions the data showed a binding trend which consisted of moderate binding ($\geq$ 60%) of Cr(VI) at low levels of competing ions with a decline when the concentration of competing ion increased. The Hausmannite showed preferential binding to the Cr(III) ion in the presence of

competing ions with only a slight decrease in binding as the concentration of competing ions increased.

This research has demonstrated that the three different nanoparticles can sequester both Cr(VI) and Cr(III) in aqueous solutions, and that the synthesis are very cost effective. The materials affinity and cost make them a strong candidate for sequestering both chromium species should it become a strong concern.

References

Chapter 1

1. T.J. O'Brien, S. Ceryak and S.R. Patierno. **Complexities of chromium carcinogenesis: role of cellular**. Fundamental and Molecular Mechanisms of Mutagenesis (2003): 533 3-36
2. A. Gambelunghe, et al. **Primary DNA damage in chrome-plating workers**. Toxicology (2003): 188, 187-195.
3. W. Liu et al. **Bioenergetics and DNA alteration of normal human fibroblasts**. Environmental Toxicology and Pharmacology (2009): 58-63.
4. N.K. Chandra Babu, K. Asma, A. Raghupathi, R. Venba, R. Ramesh, S. Sadulla. **Screening of leather auxiliaries for their role in toxic hexavalent chromium formation in leather-posing potential health hazards to the users**. Journal of Cleaner Production (2005): 13 1189-1195.
5. Agency for Toxic Substances and Disease Registry. **ToxFAQs™ for Chromium**. 2008. 2 July 2010 <http://www.atsdr.cdc.gov/tfacts7.html#bookmark10>.
6. Lenntech Water treatment & purification Holding B.V. **Chromium (Cr) and water**. 2009. 2 July 2010 <http://www.lenntech.com/periodic/water/chromium/chromium-and-water.htm>.
7. K.P Nickens, S.R. Patierno, S. Ceryak. **Chromium genotoxicity: A double-edged sword**. Chemico-Biological Interactions. (2010): In Press.
8. Environmental Protection Agency. **List of Contaminants & their MCLs**. July 2010. 2 July 2010 <http://www.epa.gov/safewater/contaminants/index.html>.

9. J. Blasiak, J. Kowalik. **A comparison of the in vitro genotoxicity of tri- and hexavalent chromium**. Mutation Research. (2000): 469 135-145.
10. R. Franco, et al. **Environmental toxicity, oxidative stress and apoptosis: Ménage à Trois**. Mutation Research/Genetic Toxicology and Environmental Mutagenesis (2009): 674 3-22.
11. P. Yuan, D. Liu, M. Fan, D. Yang, R. Zhu, F. Ge, J.X. Zhu,. H. He. **Removal of hexavalent chromium [Cr(VI)] from aqueous solutions by the diatomite-supported/unsupported Magnetite nanoparticles.** Journal of Hazardous Materials (2010), 173(1-3), 614-621.
12. J. Hu, I.M.C. Lo, G. Chen. **Fast removal and recovery of Cr(VI) using surface-modified Jacobsite (MnFe2O4) nanoparticles**. Langmuir (2005): 21, 11173-11179.
13. A.F White, M.L. Peterson. **Reduction of aqueous transition metal species on the surfaces of Fe(II) -containing oxides**. Geochimica et Cosmochimica Acta. (1996) 60 3799 3814.
14. M.L. Peterson et al. **Differential redox and sorption of Cr(III/VI) on natural silicate and oxide minerals: EXAFS and XANES results**. Geochimica et Cosmochimica Acta. (1996) 61 3399-3412.
15. M. Anbia, N. Mohammadi, K. Mohammadi. **Fast and efficient mesoporous adsorbents for the separation of toxic compounds from aqueous media**. Journal of Hazardous Materials (2010): 176, 965-972.
16. O.Ajouyeda, C. Hurel, M. Ammari, L. B. Allal, N. Marmier. **Sorption of Cr(VI) onto natural iron and aluminum (oxy)hydroxides: Effects of pH, ionic strength and initial concentration**. Journal of Hazardous Materials (2009): 616–622.

17. Environmental Protection Agency. **Basic Information about Chromium in Drinking Water**. 5 March 2010. 14 July 2010 <http://www.epa.gov/safewater/contaminants/basicinformation/chromium.html#eight>.

Chapter 2

1. T.J. O'Brien , S. Ceryak and S.R. Patierno. **Complexities of chromium carcinogenesis: role of cellular**. Fundamental and Molecular Mechanisms of Mutagenesis (2003):3-36
2. Wu, Yanjun and Yifei Tong, Xinhua Xu Jinghui Zhang. **Chromium (VI) reduction in aqueous solutions by Fe_3O_4-stabilized Fe0 nanoparticles**. Journal of Hazardous Materials (2009): 1640–1645.
3. N.K. Chandra Babu, K. Asma, A. Raghupathi, R. Venba, R. Ramesh, S. Sadulla. **Screening of leather auxiliaries for their role in toxic hexavalent chromium formation in leather-posing potential health hazards to the users**. Journal of Cleaner Production (2005): 13 1189-1195.
4. W. Liu, et al. **Bioenergetics and DNA alteration of normal human fibroblasts**. Environmental Toxicology and Pharmacology (2009): 58-63.
5. Franco, Rodrigo, et al. **Environmental toxicity, oxidative stress and apoptosis: Ménage à Trois**. Mutation Research/Genetic Toxicology and Environmental Mutagenesis (2009): 674 3-22.
6. Environmental Protection Agency. **List of Contaminants & their MCLs**. July 2010. 2 July 2010 <http://www.epa.gov/safewater/contaminants/index.html>.
7. Y.F. Shen, J. Tang, Z.H. Nie, Y.D.Wang, Y. Ren, L. Zuo. **Preparation and application of magnetic Fe3O4 nanoparticles for wastewater purification**. Journal of Seperation and Purification Technology (2009), 68, 312-319.

8. P. Yuan, D. Liu, M. Fan, D. Yang, R. Zhu, F. Ge, J.X. Zhu,. H. He. **Removal of hexavalent chromium [Cr(VI)] from aqueous solutions by the diatomite-supported/unsupported Magnetite nanoparticles.** Journal of Hazardous Materials (2010), 173(1-3), 614-621.
9. P. Yuan, M. Fan, D. Yang, H. He, D. Liu, A. Yuan, J.X. Zhu, T.H Chen. **Montmorillonite-supported Magnetite nanoparticles for the removal of hexavalent chromium [Cr(VI)] from aqueous solutions.** Journal of Hazardous Materials (2009), 166(2-3), 821-829.
10. L. Wei, G. Yang, R. Wang, W. Ma. **Selective adsorption and separation of chromium (VI) on the magnetic iron–nickel oxide from waste nickel liquid**. Journal of Hazardous Materials (2009): 1159–1163.
11. J.G Parsons, C. Luna, C.E. Botez, J. Elizalde, J.L. Gardea-Torresdey. **Microwave-assisted synthesis of iron(III)oxyhydroxides/oxides characterized using transmission electron microscopy, X-ray diffraction, and X-ray absorption spectroscopy**. Journal of Physics and Chemistry of Solids (2009): 555–560.
12. N.K Lazaridis, Ch. Charalambous. **Sorptive removal of trivalent and hexavalent chromium from binary aqueous solutions by composite alginate–goethite beads**. Water Research (2005):39 4385–4396.
13. O.Ajouyeda, C. Hurel, M. Ammari, L. B. Allal, N. Marmier. **Sorption of Cr(VI) onto natural iron and aluminum (oxy)hydroxides: Effects of pH, ionic strength and initial concentration**. Journal of Hazardous Materials (2009): 616–622.

14. J. M Zachara, D.C. Girvin, R.L. Schmidt, C. Thomas. **Chromate adsorption on amorphous iron oxyhydroxide in the presence of major groundwater ions.** Environ. Sci. Technol. (1987), *21,* 589-594.

15. M.S Gasser, GH.A. Morad, H.F. Aly. **Batch kinetics and thermodynamics of chromium ions removal from waste solutions using synthetic adsorbents**. Journal of Hazardous Materials (2007): 142, 118–129.

16. E. Smith, K. Ghiassi. **Chromate removal by an iron sorbent: mechanism and modeling**. Water Environment. Research. (2006), 78(1), 84-93.

17. P. Wang, I.M.C. Lo. **Synthesis of mesoporous magnetic γ -Fe2O3 and its application to Cr(VI) removal from contaminated water.** Water Research (2009), 43(15), 3727-3734.

18. Y. Li et al.. **Hexavalent chromium removal from aqueous solution by adsorption on aluminum magnesium mixed hydroxide**. Water Research, (2009), 43(12), 3067-3075.

19. Z.L. Zhu, L.G. Kong, H.M. Ma, J.F. Zhao,. **Adsorption of chromium (VI) on two iron (hydr)oxides.** Yingyong Huaxue (2007) 24(8), 933-936.

20. H. Fukuoka, N. Shigemoto, H. Inomo, W. Shiraki,. **Chromate adsorption on iron oxyhydroxides with different crystal forms in the presence of soil materials.** Journal of Chemical Engineering of Japan (2008), 41(2), 69-75.

21. Liu, J. C.; Huang, J. G. **Using iron-coated spent catalyst as an alternative adsorbent to remove Cr(VI) from water**. Water Science. Technology. (1998), 38(4-5), 155-162.

22. Dinesh Mohana, Charles U. Pittman Jr. **Activated carbons and low cost adsorbents for remediation of tri- and hexavalent chromium from water**. Journal of Hazardous Materials. (2006) 137 762-811.

23. V.K. Gupta, A. Rastogi, A. Nayak. **Adsorption studies on the removal of hexavalent chromium from aqueous solution using a low cost fertilizer industry waste material.** Journal of Colloid and Interface Science (2010): 342 135-141.

24. Z. Sadaoui S. Hemidouche, O. Allalou. Removal of hexavalent chromium from aqueous solutions by micellar compounds. Desalination. (2009) 249 768-773.

25. F. Magalhães, M.C. Pereira, J.D. Fabris, S.E.C. Bottrel , M.T.C. Sansiviero, A. Amayab, N. Tancredi b, R.M. Lago. **Novel highly reactive and regenerable carbon/iron composites prepared from tar and hematite for the reduction of Cr(VI) contaminant**. Journal of Hazardous Materials. (2009): 1016–1022.

26. J. Hu, I. M.C. Lo, G. Chen. **Comparative study of various magnetic nanoparticles for Cr(VI) removal**. Separation and Purification Technology. (2007) 56 249-256.

27. P. Janoš, V. Hula, P. Bradnová, V. Pilarová , J. Šedlbauer. **Reduction and immobilization of hexavalent chromium with coal- and humate-based sorbents**. Chemosphere (2009): 75 732-738.

28. Deliyanni, E.A, E.N. Peleka, K.A. Matis. **Modeling the sorption of metal ions from aqueous solution by iron-based adsorbents**. Journal of Hazardous Materials. (2009): 172 550-558.

29. J.G. Parsons, M.L. Lopez, J.R. Peralta-Videa, J.L. Gardea-Torresdey. **Determination of arsenic(III) and arsenic(V) binding to microwave assisted hydrothermal synthetically prepared Fe3O4, Mn3O4, and MnFe2O4 nanoadsorbents**. Microchemical Journal (2009): 91, 100–106.

30. M. E. Fleet **The structure of Magnetite** Acta Cryst. (1981). B37, 917-920

Chapter 3

1. Y.F. Shen, J. Tang, Z.H. Nie, Y.D.Wang, Y. Ren, L. Zuo. **Preparation and application of magnetic Fe3O4 nanoparticles for wastewater purification**. Journal of Seperation and Purification Technology (2009), 68, 312-319.
2. P. Yuan, D. Liu, M. Fan, D. Yang, R. Zhu, F. Ge, J.X. Zhu,. H. He. **Removal of hexavalent chromium [Cr(VI)] from aqueous solutions by the diatomite-supported/unsupported Magnetite nanoparticles.** Journal of Hazardous Materials (2010), 173(1-3), 614-621.
3. P. Yuan, M. Fan, D. Yang, H. He, D. Liu, A. Yuan, J.X. Zhu, T.H Chen. **Montmorillonite-supported Magnetite nanoparticles for the removal of hexavalent chromium [Cr(VI)] from aqueous solutions.** Journal of Hazardous Materials (2009), 166(2-3), 821-829.
4. N.K Lazaridis, Ch. Charalambous. **Sorptive removal of trivalent and hexavalent chromium from binary aqueous solutions by composite alginate–goethite beads**. Water Research (2005):39 4385–4396.
5. O.Ajouyeda, C. Hurel, M. Ammari, L. B. Allal, N. Marmier. **Sorption of Cr(VI) onto natural iron and aluminum (oxy)hydroxides: Effects of pH, ionic strength and initial concentration**. Journal of Hazardous Materials (2009): 616–622.
6. J. Hu, I.M.C. Lo, G. Chen. **Fast removal and recovery of Cr(VI) using surface-modified Jacobsite (MnFe2O4) nanoparticles**. Langmuir (2005): 21, 11173-11179.
7. M. Anbia, N. Mohammadi, K. Mohammadi. **Fast and efficient mesoporous adsorbents for the separation of toxic compounds from aqueous media**. Journal of Hazardous Materials (2010): 176, 965-972.

8. J.G Parsons, C. Luna, C.E. Botez, J. Elizalde, J.L. Gardea-Torresdey. **Microwave-assisted synthesis of iron(III)oxyhydroxides/oxides characterized using transmission electron microscopy, X-ray diffraction, and X-ray absorption spectroscopy**. Journal of Physics and Chemistry of Solids (2009): 555–560.

9. L. Wei, G. Yang, R. Wang, W. Ma. **Selective adsorption and separation of chromium (VI) on the magnetic iron–nickel oxide from waste nickel liquid**. Journal of Hazardous Materials (2009): 1159–1163.

10. J.G. Parsons, M.L. Lopez, J.R. Peralta-Videa, J.L. Gardea-Torresdey. **Determination of arsenic(III) and arsenic(V) binding to microwave assisted hydrothermal synthetically prepared Fe3O4, Mn3O4, and MnFe2O4 nanoadsorbents**. Microchemical Journal (2009): 91, 100–106.

11. S.L. Kuo, J.F. Lee, N.L. Wu. **Study on pseudocapacitance mechanism of aqueous MnFe2O4 supercapacitor.** Journal of The Electrochemical Society. (2007): A34-A38.

12. J. M Zachara, D.C. Girvin, R.L. Schmidt, C. Thomas. **Chromate adsorption on amorphous iron oxyhydroxide in the presence of major groundwater ions.** Environmental Science and Technology. (1987), *21,* 589-594.

13. M.S Gasser, GH.A. Morad, H.F. Aly. **Batch kinetics and thermodynamics of chromium ions removal from waste solutions using synthetic adsorbents**. Journal of Hazardous Materials (2007): 142, 118–129.

14. Z. Ai, Y. Cheng, L. Zhang, J. Qui. **Effcient removal of Cr(VI) from aqueous solution with Fe@Fe2O3 core-shell nanowires**. Environ. Sci. Technol. (2008) 42, 6955-6960.

15. P. Wang, I.M.C. Lo. **Synthesis of mesoporous magnetic γ -Fe2O3 and its application to Cr(VI) removal from contaminated water.** Water Research (2009), 43(15), 3727-3734.

16. Z.L. Zhu, L.G. Kong, H.M. Ma, J.F. Zhao. **Adsorption of chromium (VI) on two iron (hydr)oxides.** Yingyong Huaxue (2007), 24(8), 933-936.

17. H. Fukuoka, N. Shigemoto, H. Inomo, W. Shiraki. **Chromate adsorption on iron oxyhydroxides with different crystal forms in the presence of soil materials.** Journal of Chemical Engineering of Japan (2008), 41(2), 69-75.

Chapter 4

1. Y.F. Shen, J. Tang, Z.H. Nie, Y.D.Wang, Y. Ren, L. Zuo. **Preparation and application of magnetic Fe_3O_4 nanoparticles for wastewater purification**. Journal of Separation and Purification Technology (2009), 68, 312-319.

2. P. Yuan, D. Liu, M. Fan, D. Yang, R. Zhu, F. Ge, J.X. Zhu,. H. He. **Removal of hexavalent chromium [Cr(VI)] from aqueous solutions by the diatomite-supported/unsupported Magnetite nanoparticles.** Journal of Hazardous Materials (2010), 173(1-3), 614-621.

3. P. Yuan, M. Fan, D. Yang, H. He, D. Liu, A. Yuan, J.X. Zhu, T.H Chen. **Montmorillonite-supported Magnetite nanoparticles for the removal of hexavalent chromium [Cr(VI)] from aqueous solutions.** Journal of Hazardous Materials (2009), 166(2-3), 821-829.

4. N.K Lazaridis, Ch. Charalambous. **Sorptive removal of trivalent and hexavalent chromium from binary aqueous solutions by composite alginate–goethite beads**. Water Research (2005):39 4385–4396.
5. J. Hu, I.M.C. Lo, G. Chen. **Fast removal and recovery of Cr(VI) using surface-modified Jacobsite (MnFe2O4) nanoparticles**. Langmuir (2005): 21, 11173-11179.
6. M. Anbia, N. Mohammadi, K. Mohammadi. **Fast and efficient mesoporous adsorbents for the separation of toxic compounds from aqueous media**. Journal of Hazardous Materials (2010): 176, 965-972.
7. S. Mallick, S.S. Dash, K.M. Parida. **Adsorption of hexavalent chromium on manganese nodule leached residue obtained from NH3-SO2 leaching**. Journal of Colloid and Interface Science (2006): 297 419-425.
8. O.Ajouyeda, C. Hurel, M. Ammari, L. B. Allal, N. Marmier. **Sorption of Cr(VI) onto natural iron and aluminum (oxy)hydroxides: Effects of pH, ionic strength and initial concentration**. Journal of Hazardous Materials (2009): 616–622.
9. P. Janoš, V. Hula, P. Bradnová, V. Pilarová , J. Šedlbauer. **Reduction and immobilization of hexavalent chromium with coal- and humate-based sorbents**. Chemosphere (2009): 75 732-738.
10. J.G Parsons, C. Luna, C.E. Botez, J. Elizalde, J.L. Gardea-Torresdey. **Microwave-assisted synthesis of iron(III)oxyhydroxides/oxides characterized using transmission electron microscopy, X-ray diffraction, and X-ray absorption spectroscopy**. Journal of Physics and Chemistry of Solids (2009): 555–560.
11. J.G. Parsons, M.L. Lopez, J.R. Peralta-Videa, J.L. Gardea-Torresdey. **Determination of arsenic(III) and arsenic(V) binding to microwave assisted hydrothermal**

synthetically prepared Fe3O4, Mn3O4, and MnFe2O4 nanoadsorbents. Microchemical Journal (2009): 91, 100–106.

12. J. Yoon, E. Shim, S. Bae. H. Joo. **Application of immobilized nanotubular TiO2 electrode for photocatalytic hydrogen evolution: Reduction of hexavalent chromium (Cr(VI)) in water**. Journal of Hazardous Materials (2009): 161 1069-1074.
13. M.S Gasser, GH.A. Morad, H.F. Aly. **Batch kinetics and thermodynamics of chromium ions removal from waste solutions using synthetic adsorbents**. Journal of Hazardous Materials (2007): 142, 118–129.
14. J. Kyziol-Komosinska, F. Barba, P. Callejas, C. Rosik-Dulewska. **Beidellite and other natural low-cost sorbents to remove chromium and cadmium from water and wastewater**. Boletin De La Sociedad Española De Cerámica y Vidrio (2010) 49(2) 121-128.
15. F. Granados-Correa, J. Jiménez-Becerril. **Chromium (VI) adsorption on boehmite**. Journal of Hazardous Materials (2009): 162 1178-1184.
16. P. Wang, I.M.C. Lo, **Synthesis of mesoporous magnetic γ -Fe2O3 and its application to Cr(VI) removal from contaminated water.** Water Research (2009), 43(15), 3727-3734.
17. Z.L. Zhu, L.G. Kong, H.M. Ma, J.F. Zhao,. **Adsorption of chromium (VI) on two iron (hydr)oxides.** Yingyong Huaxue (2007) 24(8), 933-936.
18. H. Fukuoka, N. Shigemoto, H. Inomo, W. Shiraki,. **Chromate adsorption on iron oxyhydroxides with different crystal forms in the presence of soil materials.** Journal of Chemical Engineering of Japan (2008), 41(2), 69-75.

Chapter 5

1. A.F White, M.L. Peterson. **Reduction of aqueous transition metal species on the surfaces of Fe(II) -containing oxides**. Geochimica et Cosmochimica Acta. (1996) 60 3799 3814.
2. M.L. Peterson et al. **Differential redox and sorption of Cr(III/VI) on natural silicate and oxide minerals: EXAFS and XANES results**. Geochimica et Cosmochimica Acta. (1996) 61 3399-3412.
3. J. Hu, I.M.C. Lo, G. Chen. **Fast removal and recovery of Cr(VI) using surface-modified Jacobsite (MnFe2O4) nanoparticles**. Langmuir (2005): 21, 11173-11179.

Curriculum Vitae

Jeffrey Edward Hernandez was born on July 18, 1985 to Margarita Lopez and Jesus Eduardo Hernandez in El Paso Texas. In August of 2003 Jeffrey entered in to the University of Texas-El Paso. During his undergraduate studies, Jeffrey worked under the guidance of Dr. Geoffrey Saupe in the field of analytical chemistry. The project that he worked was Evaluation of a New Porous Titanium-Niobium Mixed Oxide for Photocatalytic Water Decontamination, in which he assisted his graduate student in synthesis of the materials. In addition to his studies Jeffrey was a peer leader working for Dr. James Becvar. While working as a peer leader, Jeffrey and a group of fellow peer leaders helped Dr. Becvar achieve the Star Award for the "Peer Leader Program in Chemistry at the University of Texas at El Paso" from the Texas Higher Education Coordinating Board. On December 15th of 2007 Jeffrey graduated with his bachelor of science in chemistry and a minor in physics. He was awarded the Outstanding American Chemical Society Student Affiliates award. On August of 2008, Jeffrey entered the chemistry graduate program in order to obtain his Master of Science degree in Analytical/Environmental Chemstry under the supervision and mentorship of Dr. Jorge Gardea-Torresdey, chairman of the chemistry department. During his graduate studies, Jeffrey was given his masters project, which was to study the sequestering effects of iron and manganese oxide nanomaterials on both Cr(VI) and Cr(III). While working on his project he collaborated with colleagues and authored and coauthored scientific findings for publication. Additionally he presented findings at national and regional conferences in the forms poster and oral presentations.

Oral Presentation

Hernandez, J., Gonzalez, C.M., Parsons, J.G., Gardea-Torresdey, J.L. "**Sorption of Cr(III) and Cr(VI) to high and low pressure nano-Magnetite particles (Fe3O4)"**, National SACNAS Conference, Dallas, Texas, October 14-18, 2009.

Poster Presentations

Hernandez, Jeffrey, Christina M. Gonzalez, Jason G. Parsons, Jorge L. Gardea-Torresdey, "**Sorption of Cr(III) and Cr(VI) to high and low pressure nano-Magnetite particles (Fe3O4)"**, 65th ACS Southwest Regional Meeting, El Paso, TX, November 4 – 7, 2009.

Hernandez, Jeffrey, Marisa Galan, Myrna Calderon, Walter Dickson, Hugo Alarcón, Daniel Dominquez, Yoon Kim, Rafael Ordoñez, Omar Khateeb, Albert Padilla, Lance Williams, Gina Carballo, Ahlam Azam, and Arturo Montes, **"Explorations: Teaching Students to Develop the Important Questions: 'By Jove, the Whys (wise) have it!!'",** 2006 Peer-Led Team Learning National Conference, University of Houston-Downtown, Houston TX, April 20 – 23, 2006

Dickson, Walter E., Jeffrey Hernandez, and James Becvar, "**Motivation by Nerds® and Airheads®"**, 2006 Peer-Led Team Learning National Conference, University of Houston-Downtown, Houston, TX, April 20 – 23, 2006.

Permanent Address

11736 Bunky Henry

El Paso, TX 79936

This Thesis was typed by Jeffrey Edward Hernandez